IMPROVED DESIGN OF TUNNEL SUPPORTS: VOLUME 2 - ASPECTS OF YIELDING IN GROUND-STRUCTURE INTERACTION

Charles W. Schwartz
Amr S. Azzouz
Herbert H. Einstein

MASSACHUSETTS INSTITUTE OF TECHNOLOGY
Department of Civil Engineering
Cambridge MA   02139

JUNE 1980
FINAL REPORT

HE
18.5
.A37
no.
DT-
SC-
UMTA-
0-27.II
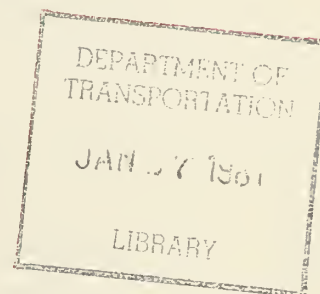
1. Report No. UMTA-MA-06-0100-80-5	2. Government Accession No.	3. Recipient's Catalog No.
4. Title and Subtitle IMPROVED DESIGN OF TUNNEL SUPPORTS: VOLUME 2 - ASPECTS OF YIELDING IN GROUND- STRUCTURE INTERACTION		5. Report Date June 1980
		6. Performing Organization Code
7. Author's) C.W. Schwartz, A.S. Azzouz, H.H. Einstein		8. Performing Organization Report No. DOT-TSC-UMTA-80-27.II
9. Performing Organization Name and Address Massachusetts Institute of Technology* Department of Civil Engineering Cambridge MA 02139		10. Work Unit No. (TRAIS) UM048/R0720
		11. Contract or Grant No. DOT-TSC-1489
12. Sponsoring Agency Name and Address U.S. Department of Transportation Urban Mass Transportation Administration Office of Technology Development & Deployment Office of Rail & Construction Technology Washington DC 20590		13. Type of Report and Period Covered Final Report (Vol. 2) January 1978-August 1979
		14. Sponsoring Agency Code

DEPARTMENT OF
TRANSPORTATION
JUN 7 1981
LIBRARY

15. Supplementary Notes *Under contract to:	U.S. Department of Transportation Research and Special Programs Administration Transportation Systems Center Cambridge MA 02142

16. Abstract

Volume 2 concentrates on a particularly complex and often misunderstood aspect of ground-structure interaction, ground yielding. Section 1 provides a conceptual review of ground yielding behavior, including outlines of appropriate analytical treatments. Emphasis is placed on the problematic phenomenon of loosening. Following the review, available methods for analyzing plastic behavior are discussed as is a detailed description of a method for analyzing strain softening ground behavior.

Volume 2 is the second of five volumes published on the Improved Design of Tunnel Supports. The Executive Summary of the five-volume report was published in December, 1979 (Report No. UMTA-MA-06-0100-79-15).

The remaining final reports published in this five-volume series are:

    Volume 1 - Simplified Analysis for Ground-Structure
              Interaction in Tunneling
    Volume 3 - Finite Element Analysis of the Peachtree Center
              Station in Atlanta
    Volume 4 - Tunneling Practices in Austria and Germany
    Volume 5 - Empirical Methods in Rock Tunneling -- Review
              and Recommendations

17. Key Words Tunneling, Support Design, Ground-Structure Interaction	18. Distribution Statement DOCUMENT IS AVAILABLE TO THE PUBLIC THROUGH THE NATIONAL TECHNICAL INFORMATION SERVICE, SPRINGFIELD, VIRGINIA 22161

19. Security Classif. (of this report) UNCLASSIFIED	20. Security Classif. (of this page) UNCLASSIFIED	21. No. of Pages 75	22. Price

Technical Report Documentation Page

1. Report No. UMTA-MA-06-0100-80-5	2. Government Accession No. PB 80-225162	3. Recipient's Catalog No.

4. Title and Subtitle	5. Report Date
IMPROVED DESIGN OF TUNNEL SUPPORTS: Volume 2 - Aspects of Yielding in Ground-Structure Interaction	June 1980
	6. Performing Organization Code
	8. Performing Organization Report No. DOT-TSC-UMTA-80-27.II

7. Author's) C. W. Schwartz, A. S. Azzouz, and H. H. Einstein

9. Performing Organization Name and Address	10. Work Unit No. (TRAIS)
Massachusetts Institute of Technology* Department of Civil Engineering Cambridge, Massachusetts 02139	MA-06-0100(UM048/R0720)
	11. Contract or Grant No. DOT-TSC-1489
	13. Type of Report and Period Covered

12. Sponsoring Agency Name and Address	Final Report Volume 2 of 5 January 1978-August 1979
U.S. Department of Transportation Urban Mass Transportation Administration 400 Seventh Street, S.W. Washington, DC 20590	14. Sponsoring Agency Code UTD-30

15. Supplementary Notes *under contract to: U.S. Department of Transportation, Research and Special Programs Administration, Transportation Systems Center, Cambridge, MA 02142. Related reports are: Executive Summary (PB 80-134547); Volume 1 (UMTA-MA-06-0100-80-4); Volume 3 (UMTA-MA-06-0100-80-6); Volume 4 (UMTA-MA-06-0100-80-7); and Volume 5 (UMTA-MA-06-0100-80-8).

16. Abstract

This five-volume report includes the results of an extensive research effort by the Massachusetts Institute of Technology to improve the design methodologies available to tunnel designers. The purpose of this report is to provide the tunneling profession with improved practical tools in the technical or design area, which provide more accurate representations of the ground-structure interaction in tunneling. The design methods range from simple analytical and empirical methods to sophisticated finite element techniques as well as an evaluation of tunneling practices in Austria and Germany.

Volume 2 focuses on a particularly complex and often misunderstood aspect of ground-structure interaction, which is ground yielding and loosening, and reports new findings in this area. The findings are based on previous research, on the knowledge gained during the development of the simplified analysis and the application of the more sophisticated finite element techniques, and on specific studies of strain softening ground behavior. A conceptual review of ground yielding behavior, including outlines of appropriate analytical treatments, is addressed in the report and emphasis is placed on the problematic phenomenon of loosening. In addition to providing some basic concepts of ground yielding, the report also describes and compares analytical solutions for plastic ground behavior. Finally, an analytical tool for treating strain softening behavior is provided. The authors point out that it is hoped that ground-yielding, and consequently, ground-structure interaction, can be better understood and analytically treated, even if some aspects remain somewhat problematic.

17. Key Words	18. Distribution Statement
Ground Loosening; Ground-Structure Interaction; Ground Yielding; Support Design; Tunnel Design; Tunnel Support; Tunneling; Underground Construction; Tunnels and Tunneling	Available to the public through the National Technical Information Service, Springfield, Virginia 22161

19. Security Classif. (of this report) Unclassified	20. Security Classif. (of this page) Unclassified	21. No. of Pages 79	22. Price A05

Form DOT F 1700.7 (8-72)   Reproduction of completed page authorized

PREFACE

This report is the second of five publications (the Executive Summary of this five-volume report was published in December, 1979) which include the results of an extensive research effort by the Massachusetts Institute of Technology (MIT) to improve the design methodologies available to tunnel designers. The contract, DOT-TSC-1489, was funded by the U.S. Department of Transportation (DOT) and was sponsored by the Urban Mass Transportation Administration's (UMTA) Office of Rail and Construction Technology. The contract was monitored by the Transportation Systems Center (TSC) Construction and Engineering Branch.

Volume 2 focuses on the complex and often misunderstood aspects of ground structure interaction, that of ground yielding. In addition to providing the reader with some basic concepts of ground yielding, the report also describes and compares analytical solutions for plastic ground behavior. Finally an analytical tool for treating strain softening behavior is provided.

The authors would like to acknowledge Mr. J. Germaine, Research Assistant, for the ideas and assistance he provided to the theoretical development of Section 3 in this volume.

METRIC CONVERSION FACTORS

Approximate Conversions to Metric Measures

Symbol	When You Know	Multiply by	To Find	Symbol
		LENGTH		
in	inches	*2.5	centimeters	cm
ft	feet	30	centimeters	cm
yd	yards	0.9	meters	m
mi	miles	1.6	kilometers	km
		AREA		
in^2	square inches	6.5	square centimeters	cm^2
ft^2	square feet	0.09	square meters	m^2
yd^2	square yards	0.8	square meters	m^2
mi^2	square miles	2.6	square kilometers	km^2
	acres	0.4	hectares	ha
		MASS (weight)		
oz	ounces	28	grams	g
lb	pounds	0.45	kilograms	kg
	short tons (2000 lb)	0.9	tonnes	t
		VOLUME		
tsp	teaspoons	5	milliliters	ml
Tbsp	tablespoons	15	milliliters	ml
fl oz	fluid ounces	30	milliliters	ml
c	cups	0.24	liters	l
pt	pints	0.47	liters	l
qt	quarts	0.95	liters	l
gal	gallons	3.8	liters	l
ft^3	cubic feet	0.03	cubic meters	m^3
yd^3	cubic yards	0.76	cubic meters	m^3
		TEMPERATURE (exact)		
°F	Fahrenheit temperature	5/9 (after subtracting 32)	Celsius temperature	°C

*1 in = 2.54 (exactly). For other exact conversions and more detailed tables, see NBS Misc. Publ. 286, Units of Weights and Measures, Price $2.25, SD Catalog No. C13.10 286.
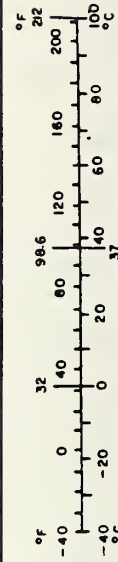
Approximate Conversions from Metric Measures

Symbol	When You Know	Multiply by	To Find	Symbol
		LENGTH		
mm	millimeters	0.04	inches	in
cm	centimeters	0.4	inches	in
m	meters	3.3	feet	ft
m	meters	1.1	yards	yd
km	kilometers	0.6	miles	mi
		AREA		
cm^2	square centimeters	0.16	square inches	in^2
m^2	square meters	1.2	square yards	yd^2
km^2	square kilometers	0.4	square miles	mi^2
ha	hectares (10,000 m^2)	2.5	acres	
		MASS (weight)		
g	grams	0.035	ounces	oz
kg	kilograms	2.2	pounds	lb
t	tonnes (1000 kg)	1.1	short tons	
		VOLUME		
ml	milliliters	0.03	fluid ounces	fl oz
l	liters	2.1	pints	pt
l	liters	1.06	quarts	qt
l	liters	0.26	gallons	gal
m^3	cubic meters	35	cubic feet	ft^3
m^3	cubic meters	1.3	cubic yards	yd^3
		TEMPERATURE (exact)		
°C	Celsius temperature	9/5 (then add 32)	Fahrenheit temperature	°F

iv

TABLE OF CONTENTS

LIST OF ILLUSTRATIONS

1. INTRODUCTION

Research into the improved design and construction of under-
ground openings is closely tied to the understanding of ground-
structure interaction. Comprehension of ground-structure inter-
action is an absolute necessity in the development of an optimum
tunneling system and especially in the derivation of appropriate
analysis and design methods. On the other hand, work on the anal-
ysis and design methods and the review of modern tunneling systems
has in turn contributed to a better understanding of various
aspects of ground-structure interaction. In other words,
principles and details of ground-structure interaction permeate
this entire series of reports (and previous work, Einstein et al.
1977).

Basically, it would be possible to get a better understanding of
ground-structure interaction in tunneling by reading through all
of these reports. However, it seems appropriate to provide the
design profession with a more explicit and summarized review on
ground-structure interaction, emphasizing some of the complex
phenomena and providing insight into some of the more controversal
aspects. Previous work (Einstein et al. 1977, Ch. 8) attempted
to review in conceptual terms the entire ground-structure inter-
action phenomenon; it also highlighted the most important factors
that needed to be taken into consideration in the development
of analytical and empirical design methods (Vols. 1, 3 and 5 of
this report series). The discussion in this volume will concen-
trate on a particularly complex and often ill understood aspect

of ground-structure interaction, that of ground yielding. The reader will be first given a conceptual review of ground yielding behavior, including outlines of appropriate analytical treatments. Emphasis will be placed on the problematic phenomenon of loosening. This will be followed by an overview of the available methods for analyzing plastic behavior and, in particular, by a detailed description of a method for analyzing strain softening ground behavior. By addressing this relatively limited but crucial aspect of ground yielding, the reader will, together with previous information provided by the authors, obtain an improved understanding of ground-structure interaction in tunneling.

2. QUALITATIVE BEHAVIOR OF YIELDING GROUND MASSES SURROUNDING TUNNELS

2.1 CHARACTERISTIC CURVE FOR A YIELDING GROUND MASS

The excavation of a tunnel results in a partial or complete unloading of the initially stressed ground mass. The stages in this unloading behavior can be conceptually illustrated by using the idealized load-displacement curve, the ground characteristic curve. The ground characteristic curve shown in Figure 2.1 has been developed by first assuming that an unlined tunnel exists in the undistrubed ground mass. This opening has an initial internal pressure, P_I, equal to the in situ ground stress. Upon gradual reduction of the internal pressure (i.e., unloading), inward radial displacement , u, of the tunnel wall occurs. The plot of internal pressure versus radial displacement is the ground characteristic curve.

There are three main stages of the unloading behavior: (1) As the internal cavity pressure is gradually reduced, the ground first responds elastically; the characteristic curve is linear during this stage. (2) At some point, yielding begins as the shear strength of the ground is exceeded at the cavity wall; the characteristic curve becomes distinctly nonlinear during this stage. (3) Finally, under some conditions continued deformations may lead to an unstable situation in which the internal cavity pressure must be increased to maintain a given ground
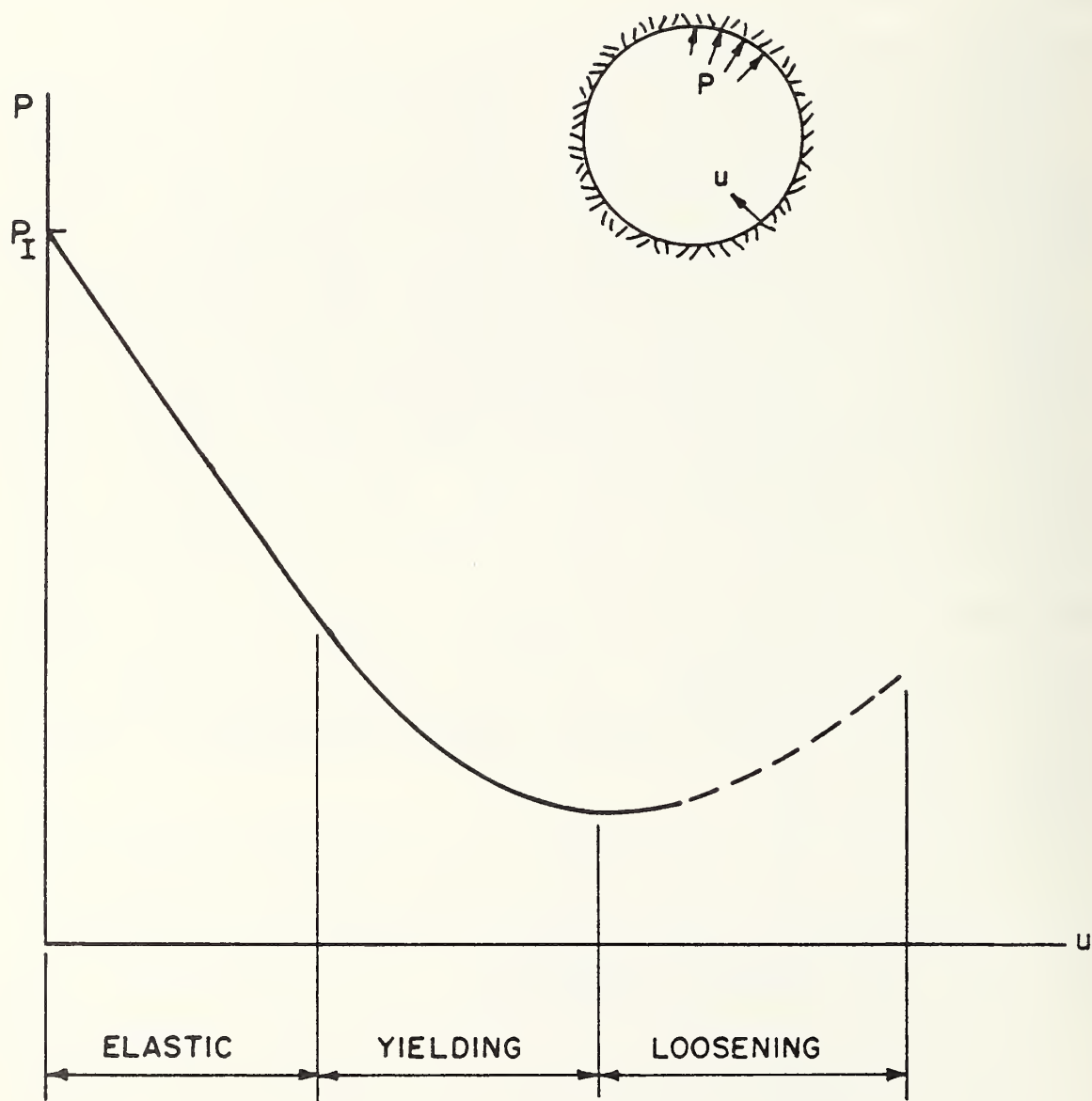
FIGURE 2.1.   GROUND CHARACTERISTIC CURVE

displacement; the characteristic curve sweeps upward in this loosening stage.

True elastic behavior is generally limited to intact rock or homogeneous soil deposits over a limited stress range. Layered soils and discontinuous rock masses can often be approximated by an anisotropic elastic medium for small stress changes. If the ground mass were truly elastic over all stress ranges, the ground characteristic curve would be a straight line and the opening would be stable even at zero internal pressure.

Yielding occurs as soon as the failure strength of the ground is exceeded either within a continuous soil mass or rock block or along a discontinuity (rock joint, fault, or other weakness plane). The eventual stability of the opening depends heavily on the post-failure behavior of the ground mass. Cavities in perfectly plastic or strain hardening grounds with a cohesive strength component will always stabilize at zero internal pressure, although the concomitant radial displacements of the cavity wall may be very large. Severely strain softening ground, on the other hand, will require a positive internal pressure or counterstress to maintain stability. The loosening range of the ground characteristic curve is commonly associated with this strain softening ground behavior (this will be further discussed in Section 2.4).

2.2 FAILURE BEHAVIOR OF THE GROUND

A simplified example of the stress conditions around a tunnel that could lead to ground failure is illustrated in Figure 2.2. The elastic stresses on typical crown and springline elements at
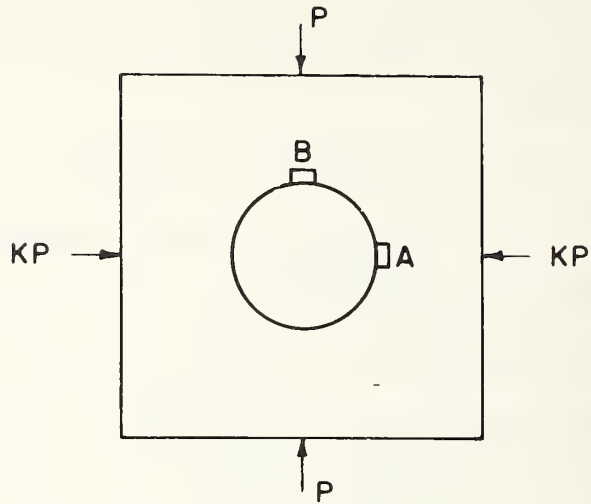
(a) AT SPRINGLINE (ELEMENT A)
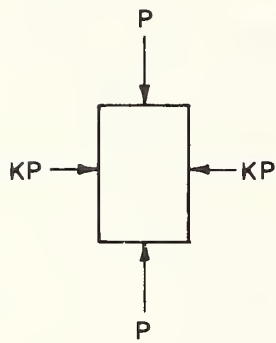
Before Excavation

After Excavation

(b) AT CROWN (ELEMENT B)

Before Excavation
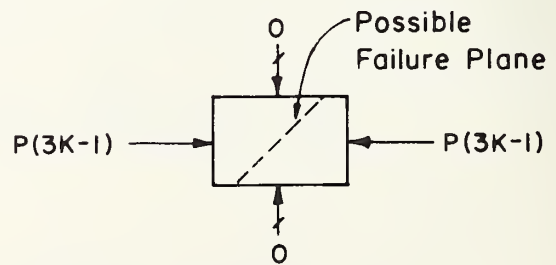
After Excavation

FIGURE 2.2. STRESS STATES AT TUNNEL WALL

6

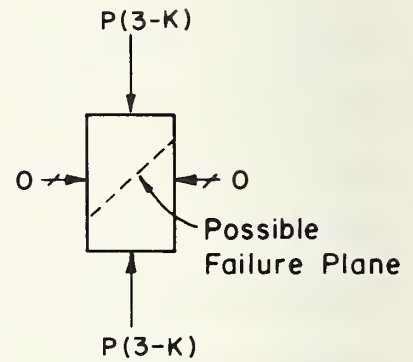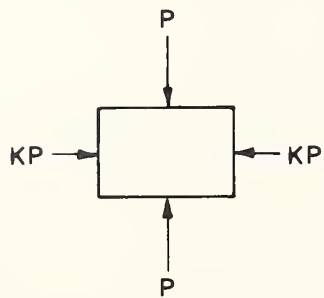the wall of an unlined tunnel are shown. Before excavation, the stresses on the elements are simply the in situ ground stresses. After excavation, the circumferential (tangential) stresses greatly increase while the radial or "confining" stresses drop to zero. If the circumferential stresses are large enough, failure along the indicated inclined planes is possible.

The post-failure behavior of the ground elements at the tunnel wall can be studied by considering an idealized triaxial test, as shown in Figure 2.3a. The axial stress, σ_1, corresponds to the tangential stresses in the ground, while the lateral confining pressure, σ_3, corresponds to the applied radial pressure (or support pressure) at the cavity wall. As the internal pressure in the tunnel is gradually reduced, σ_1 increases and σ_3 decreases. At some point during this unloading, the difference between σ_1 and σ_3 becomes so large that the failure strength of the material is exceeded.

After failure occurs in the ground mass, it becomes difficult to qualitatively predict the changes in σ_1 and σ_3. The overall stress distributions in the yielded ground mass are largely dependent upon its post-failure constitutive behavior. However, for the purpose of studying the post-failure behavior of an individual element in the ground mass, it is convenient to make the very simplistic assumption that σ_1 remains constant. Although this will not generally be the case around a tunnel, it does make it
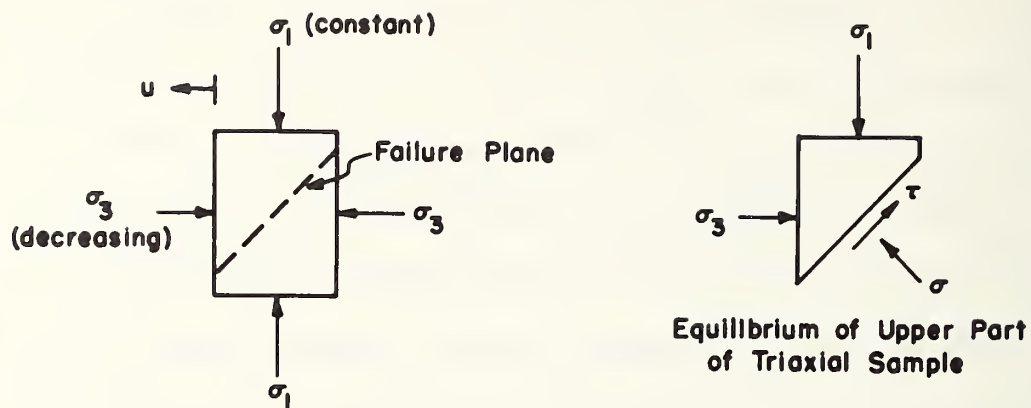
7
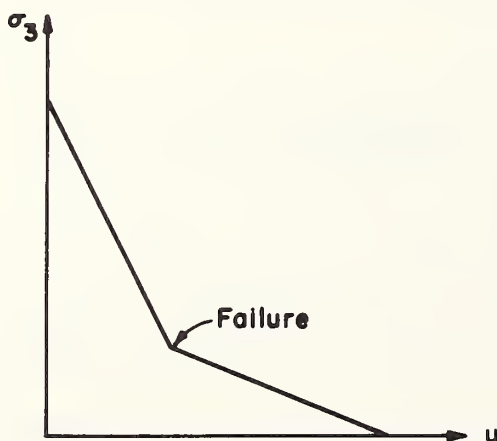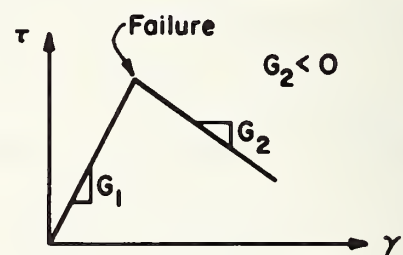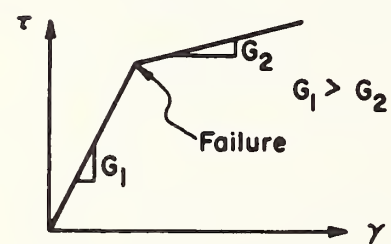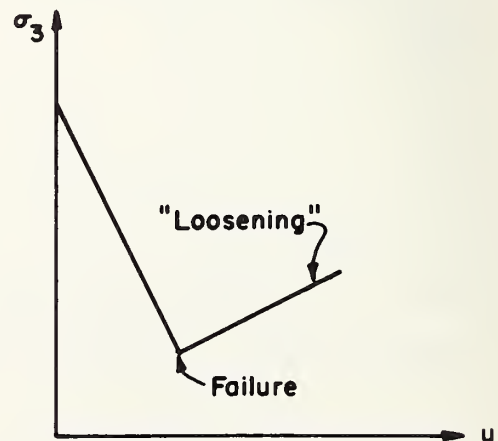
FIGURE 2.3.   POST-FAILURE GROUND BEHAVIOR

8

easier to visualize the important features of strain harden-
ing and strain softening ground behavior.

If the material is strain hardening (Figure 2.3b), it
can continue to sustain an additional stress differential
after failure. A further reduction in the lateral stress
will be balanced by an increase in shear resistance along
the failure plane. However, in this post-failure range large
shear strains are required to mobilize this additional
shear resistance. As a result, the lateral displacement,
u, of the "triaxial sample" will be much greater for a
given decrement of lateral stress after failure has occured
than before. The lateral stress can, however, eventually
be reduced to zero without causing instability.

In strain softening materials, on the other hand, the
shear stresses in the material will reach a peak at failure
and then decrease with additional shear strains (Figure 2.3c).
A reduction in the applied lateral stresses cannot now be
counteracted by increased shear resistance along the failure
plane even after very large strains have occurred; in fact,
additional post-failure shear strains result in a decrease
in the shear resistance along the failure plane. Therefore,
the applied stress differential must be reduced by increas-
ing the lateral stress (if the axial stress is held constant)
in order to compensate for this reduction in shear strength.
This increase in the lateral stress results in the upward
sloping segment of the stress-displacement curve (Figure
2.3c).

The differences between strain hardening and strain softening behavior can be viewed in another way if the ground material is assumed to follow a Mohr-Coulomb failure criterion, as illustrated in Figure 2.4. The quantities ϕ_i and c_i are the initial friction angle and cohesion of the ground, while ϕ_u and c_u are the corresponding ultimate strength parameters. In a strain hardening material (Figure 2.4a), these ultimate strength properties are larger than the initial values; therefore, the Mohr's circle at initial failure must expand to reach the ultimate condition. The principal stresses, σ_1 and σ_3, can be adjusted in an infinite number of ways to satisfy this ultimate failure criterion. However, if it is again assumed that σ_1 (the axial stress in our conceptual triaxial experiment) remains constant, it is clear that σ_3 (the lateral stress) can be reduced in the ultimate condition.

The analogous case for a strain softening material is shown in Figure 2.4b. Here, the ultimate strength parameters are less than the initial values; now the Mohr's circle for initial failure must shrink to reach the ultimate condition. If σ_1 is again assumed to remain unchanged, σ_3 must be increased in the ultimate state.

As mentioned earlier, though, the actual behavior around a tunnel is more complicated than the simple scenarios outlined above would indicate. Although the general descriptions of the failure and post-failure behavior are correct, the convenient assumptions for the stresses are
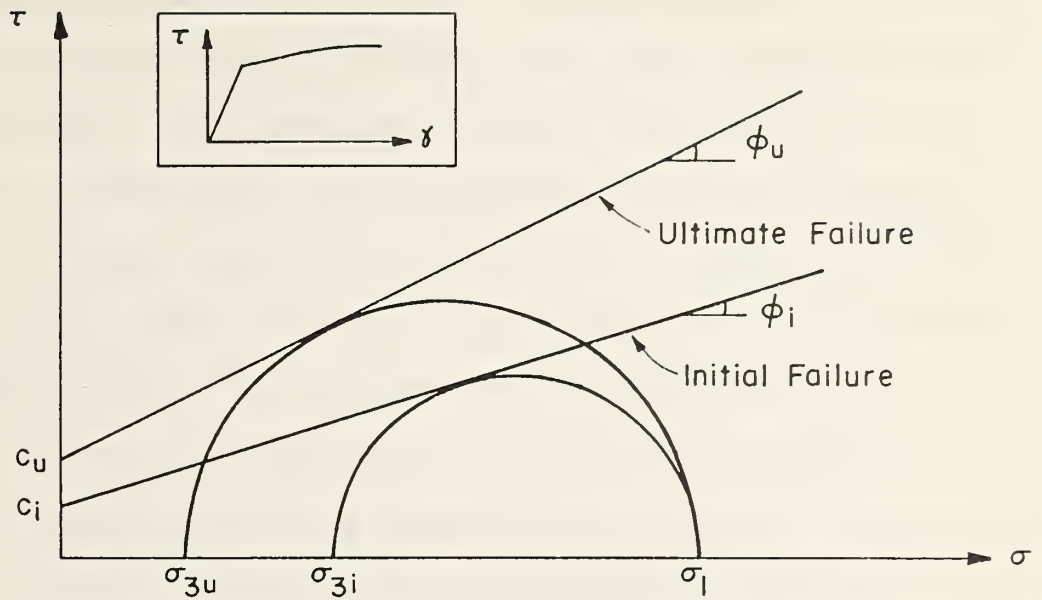
a) STRAIN HARDENING
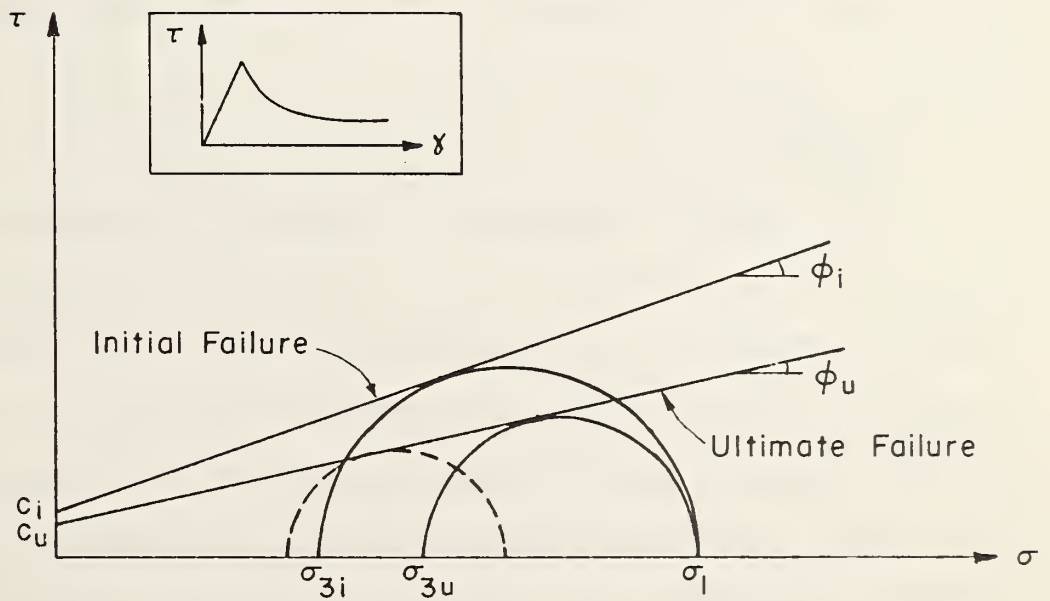
b) STRAIN SOFTENING

FIGURE 2.4.   POST-FAILURE BEHAVIOR, MOHR-COULOMB FAILURE
CRITERION

11

not. Since ground yielding leads to a stress redistribution around the tunnel, the assumption of a constant σ_1 is not generally valid for the real tunneling situation, nor are the conclusions regarding σ_3. For example, if the tangential stress σ_1 drastically drops due to the stress redistribution after failure, the radial (support) pressure σ_3 may decrease even in a severely strain softening case (see dashed Mohr's circle in Figure 2.4b); this conclusion is just the opposite of that drawn when σ_1 was held constant (solid Mohr's circle for residual conditions in Figure 2.4b). Nevertheless, even if the stresses in the yielded ground mass are not precisely known, the conceptual reasoning outlined in this section can still aid in the qualitative assessment of different types of behavior.

2.3 DILATANCY

Many geologic materials of interest in tunneling dilate as they fail; that is, the post-failure strains cause an increase in the material's volume. The degree of dilatancy exhibited by a given material depends upon many factors: the strength parameters (particularly the friction angle), confining stress, level of shear strains, and joint geometry and roughness (for rock masses) are some examples. Dilatancy merits special mention in the tunneling problem because it alters the shape of the ground characteristic curve in both the yielding and loosening ranges. Because of dilatancy, the ground within the

yielded zone will increase in volume. To accommodate

this volume increase, the tunnel wall must move radially

inward. Therefore, if it is assumed that the extent

of the yielded zone is the same for a given internal cavity

pressure regardless of whether or not dilatancy develops,

the radial displacements at the wall of a tunnel in a

strongly dilatant ground mass will be larger than those

for a tunnel in a ground that does not dilate as it yields.

These larger displacements at a given internal cavity

pressure mean that dilatancy "flattens" the ground charac-

teristic curve, as shown in Figure 2.5. Dilatancy exag-

gerates the effects of ground yielding and lessens the

effects of loosening.

2.4 LOOSENING

Loosening is defined as an increase in the internal

cavity pressure at increasing displacements of the tunnel

wall -- in other words, it is the upward sweep of the

tail of the ground characteristic curve. This concept,

formally stated by Pacher 15 years ago, is today some-

what controversial and by no means universally embraced

by the tunneling fraternity. The problem is that loosening,

besides being difficult to justify theoretically, has

never been observed in an actual tunnel. Even in tunnels

built by the New Austrian Tunneling Method (NATM), which

permits the largest ground movements and therefore pro-

duces the greatest potential for loosening, the intensive

performance monitoring has never detected an increase in

13
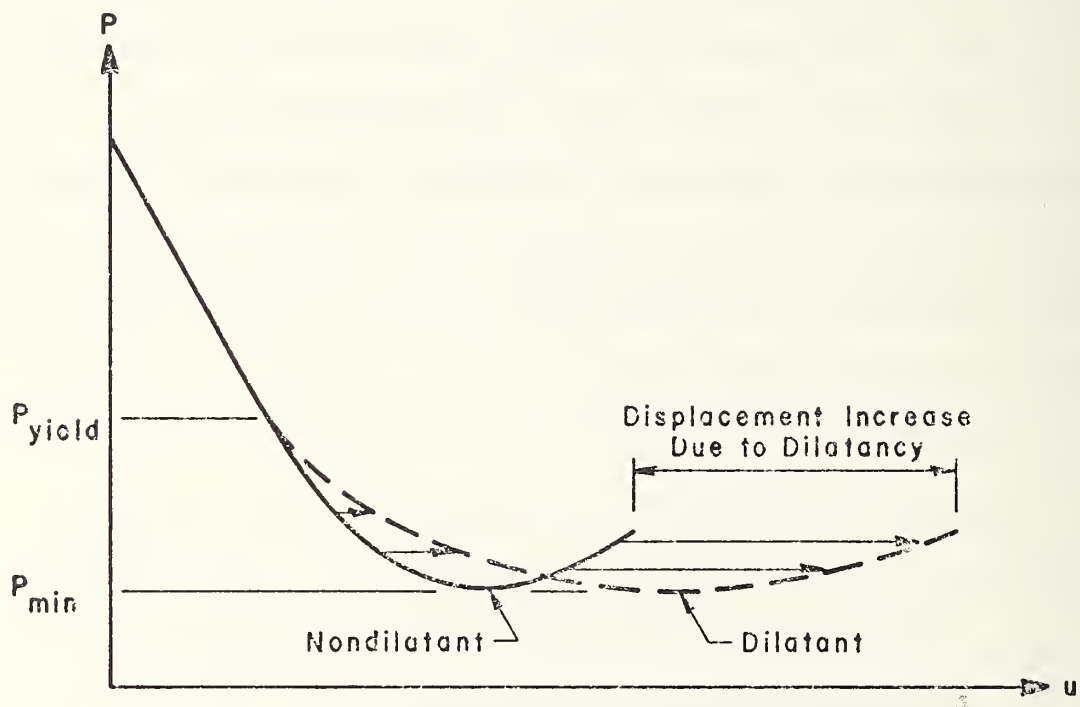
FIGURE 2.5. EFFECT OF DILATANCY ON THE GROUND CHARACTERISTIC
CURVE

14

support load with increasing displacements. Nevertheless, the theoretical possibility of loosening is still maintained by many practitioners of the NATM and other tunneling systems.

There are two schools of thought on the underlying mechanisms for loosening and will be described in the following sections. The first school treats the ground mass as a severely strain softening continuum; as the ground yields and becomes progressively less strong, it becomes unstable and a higher support pressure is required to maintain equilibrium. The second school considers loosening as an extension of arching theory; yielding in the ground mass leads to the deterioration of the ground arch above the tunnel which in turn leads to higher support loads. Both schools consider localized gravity loading (in an approximate manner) as an additional factor influencing loosening. Justification for all of these mechanisms has traditionally been based primarily on highly speculative reasoning, supplemented by some limited (and often contradictory) analytical work.

2.4.1 Loosening in a Strain Softening Continuum

The strain softening mechanism is perhaps the easier to visualize. As an individual strain softening ground element fails, its strength deteriorates and large post-failure strains develop. The overall strength of the

yielded zone thus decreases as the overall ground movements are simultaneously increasing. The effects of this behavior can be studied with the aid of the family of ground characteristic curves shown in Figure 2.6. Figure 2.6a depicts the relationship between the overall strength of the ground in the yielded zone (i.e., the average post-failure strength of all of the individual ground elements) and the radial displacement of the tunnel wall (which is a function of the average strains in all of the individual ground elements). As the deformations increase, the overall ground strength decreases -- i.e., strain softening develops. A radial displacement u_1 corresponds to the overall strength properties c_1 and ϕ_1 which in turn correspond to the ground characteristic curve C_1 in Figure 2.6b; u_2 corresponds to c_2 and ϕ_2 which produce curve C_2; and so on. The equilibirum pressure P_1 corresponding to displacement u_1 is then given by point 1 on curve C_1, P_2 at displacement u_2 is represented by point 2 on curve C_2, etc. The characteristic curve for the overall ground behavior is the locus of all these points, illustrated as the heavy dashed line in Figure 2.6b. Because of the strain softening behavior of the ground, this overall ground characteristic curve sweeps upward at large displacements.

16

a)

b)
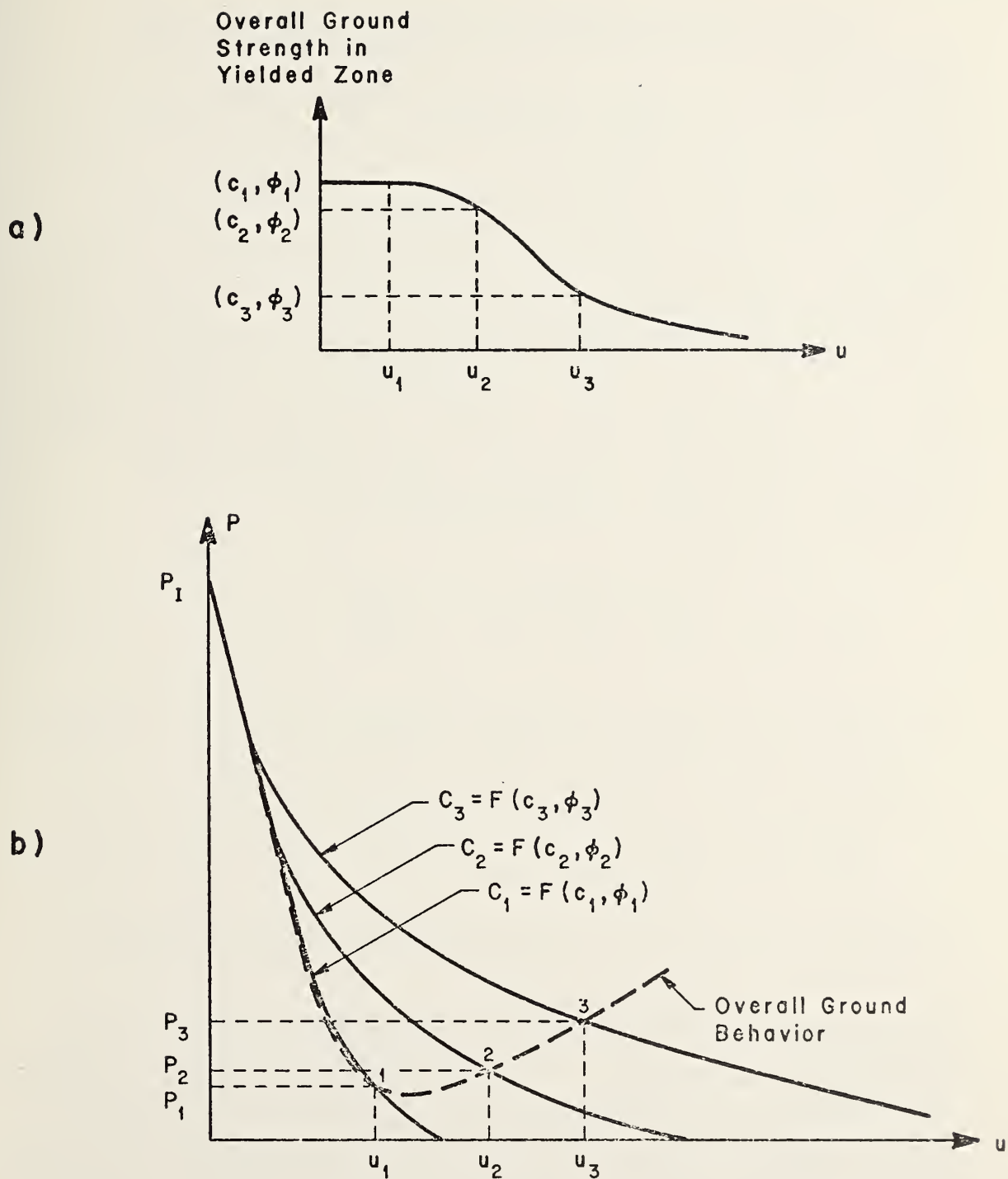
FIGURE 2.6.   CHARACTERISTIC CURVE FOR STRAIN SOFTENING GROUND BEHAVIOR

17

Several attempts have been made to analytically investigate this strain softening behavior around the tunnel, but their results have been inconsistent. Daemen (1975) calculated a ground characteristic curve similar to that in Figure 2.6 from an approximate analysis based on simple plane-strain plasticity solutions.[1] He assumed that the elastic modulus E and the strength parameters c and ϕ for the ground were constant throughout the yielded zone but that their values were approximately strain dependent, following the exponential law:

$$E_y = E_r + (E_p - E_r) \exp \left\{ -k\left[\left(\frac{b}{a}\right)^2 - 1\right] \right\} \qquad (2.1a)$$

$$c_y = c_r + (c_p - c_r) \exp \left\{ -k\left[\left(\frac{b}{a}\right)^2 - 1\right] \right\} \qquad (2.1b)$$

$$\phi_y = \phi_r + (\phi_p - \phi_r) \exp \left\{ -k\left[\left(\frac{b}{a}\right)^2 - 1\right] \right\} \qquad (2.1c)$$

in which E_y, c_y, ϕ_y = values throughout yielded zone

---

[1]This type of solution has been described in more detail in Section 4 of Volume 1 of this report. Daemen's formulation is similar to solution B.3 in that chapter. The stresses in the elastic and yielded regions are derived rigorously (in terms of plasticity theory, subject to the simplifying assumptions inherent in the solution), but the derivation of the radial displacement at the tunnel wall is based on the approximations that, in the yielded zone, the plastic volumetric strains are zero and the elastic strains are functions of the reduced modulus E_y in (2.1a).

E_r, c_r, ϕ_r = residual (minimum) values

E_p, c_p, ϕ_p = peak (maximum) values

k = a constant ranging from 0 (no strain
softening) to ∞ (abrupt drop from peak
to residual values immediately upon
yielding)

a = radius of tunnel

b = radius of yielded zone

In this formulation, Daemen makes the very rough approximation that the "typical" value for the plastic strains used to determine the strain softening ground properties is directly related to the normalized radius of the yielded zone, $\frac{b}{a}$ (in Figure 2.6a, an equally approximate assumption was made that these strains were related to the radial displacement of the tunnel wall); thus E_y, c_y, and ϕ_y can be expressed in (2.1) as functions of $\frac{b}{a}$, greatly expediting the solution. Daemen bases his calculations of the radial ground displacements on the assumption that, in the yielded zone, the plastic volumetric strains are everywhere zero and the elastic strains are computed

19

using the reduced modulus E_y.

One set of results from Daemen's analysis is shown in Figure 2.7. As expected in the case of no strain softening (k=0), no loosening develops; the ground curve decreases monotonically to a stable equilibrium at zero pressure. For increasing amounts of strain softening (increasing k), however, the ground curve changes form and loosening does indeed develop; as the ground displacements increase, the cavity pressure decreases, reaches a local minimum, increases, but then eventually decreases again. Based on Daemen's analysis, loosening is therefore a transient phenomenon. Support loads will increase for a limited range of ground movements, but increasing these movements even further will again reduce the pressures.

Unfortunately, Daemen's results display a certain inconsistency. If loosening is indeed a result of strain softening ground behavior, then why does the most strain softening case (k=∞, abrupt drop from peak to residual strength immediately upon yielding) exhibit the most loosening? In fact, this most-strain-softening case does not exhibit any loosening. Although Daemen aknowledges that the "path along which the residual properties are approached has a decisive influence upon the shape of the ground reaction [characteristic] curve" (pg. II-53), he does not really offer an explanation for

20
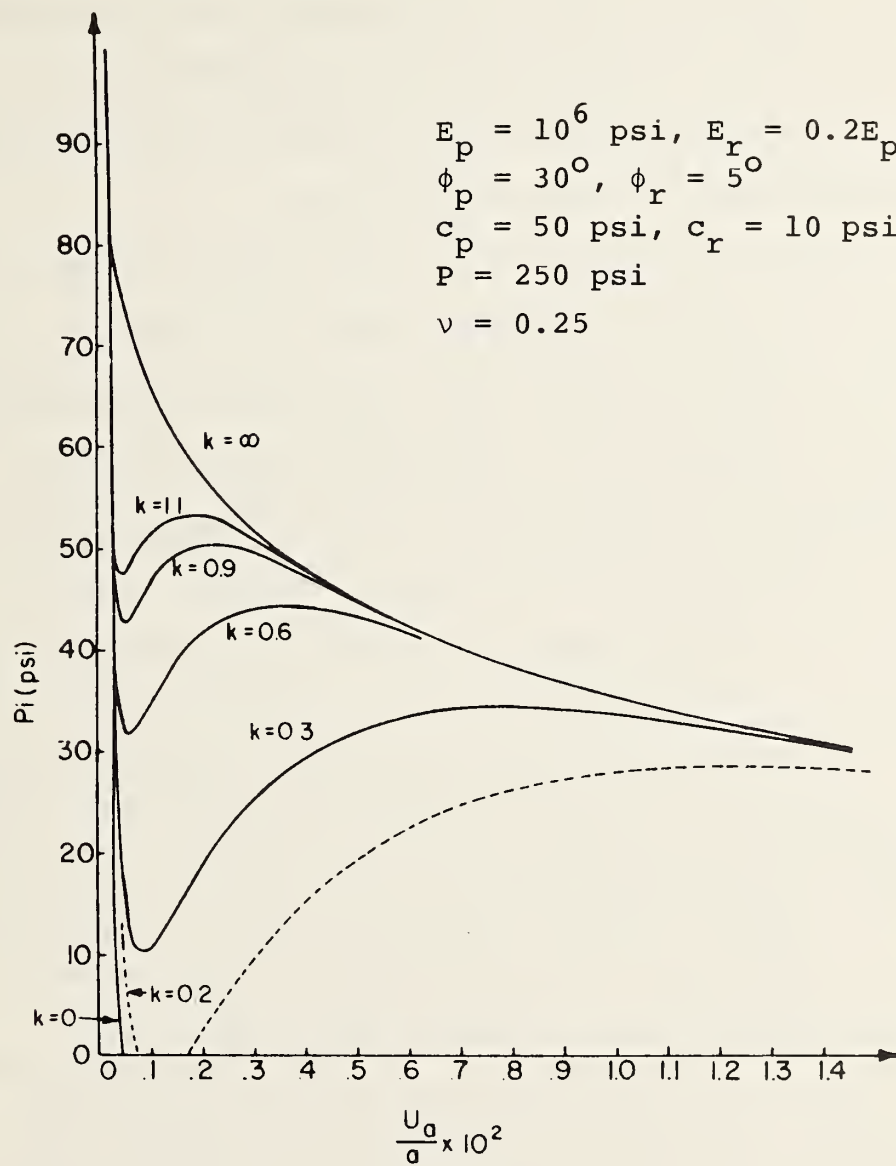
FIGURE 2.7. CHARACTERISTIC CURVES FROM DAEMEN's STRAIN
SOFTENING ANALYSIS (FROM DAEMEN, 1975)

21

this inconsistency in his results. The ground loosening calculated by Daemen probably is influenced in part by the shape of the strain softening curve, as he suggests, but it is also very likely influenced by the specific simplifying assumptions in the analysis used for the calculations.

In the following section, analytical studies on the effect of strain softening behavior will be described. Using approximate closed-form solutions, the effect of a trilinear strain softening constitutive relation (versus Daemen's "linear-exponential: formulation) on the ground yielding and loosening around a tunnel was examined for cases similar to Daemen's. No loosening behavior could be observed in any of the calculations.

In addition to strain softening ground behavior, Daemen considered, in a very approximate fashion, the effects of localized gravity loadings in his solution. Consciously ignoring the effects of the gravity body forces in the elastic zone, Daemen adds the body force term to the equilibrium equations for the strain softening yielded zone and then solves these equations along the vertical axis of symmetry (a similar and more familiar approach was developed much earlier by Fenner, 1938). For severely strain softening ground, the body force term is large relative to the other stresses and thus strongly influences the radial stresses along the vertical axis (e.g., the radial support pressure right at the crown). In

essence, this solution implies that as a severely strain softening ground yields around the tunnel, it loses nearly all of its strength and the material above the crown "falls" onto the support due to gravity forces. (The material below the invert also loses its strength, but it "falls" away from the tunnel onto the outer elastic ground zone.) Thus, this very approximate solution leads to the unsurprising conclusion that gravity forces will increase the crown loads for a tunnel in a yielding ground mass and will exacerbate the effects of loosening, should it develop.

2.4.2 Loosening as Explained by Arching Theory

Since Terzaghi's arching theory is the basis of many tunnel design methods, several attempts have been made to use it to explain the loosening phenomenon. The discussion of the arching phenomenon around tunnels requires a perspective slightly different from that in the preceding section, however. The analysis of ground yielding and loosening in terms of characteristic curves and plasticity solutions has up to this point implicitly treated the internal cavity or support pressure as the independent variable -- that is, the reduction of the internal cavity pressure caused the ground to deform, but not vice versa. However, in arching theory it is conven- ient to use the converse relationship: the deformation

23

of the ground causes a change in the internal cavity pressure needed to maintain equilibrium. Here the ground deformation is the independent variable, and the corresponding internal support pressure can be thought of as an active load on the tunnel support. Of course, the two perspectives are really equivalent since they both represent the same underlying phenomenon, but there are certain advantages to attacking the problem from different directions.

Arching above tunnels is an extension of Terzaghi's (1943) classical solution for arching of an ideal soil above a yielding trap door. The basic assumptions in the solution are (see Figure 2.8):

1) Sliding surfaces rise vertically from the edges of the trap door

2) $\sigma_v = \sigma_z$, $\sigma_h = K\sigma_v$ everywhere, K an empirical constant

3) Full shear resistance is mobilized along assumed slip surfaces

4) The vertical stress σ_v is constant across horizontal sections.

5) There are rigid support conditions at both sides of the trap door

A limiting equilibrium analysis can be performed for the situation depicted in Figure 2.8 and, if the slip lines are assumed to extend only to a height of 5B above the

24
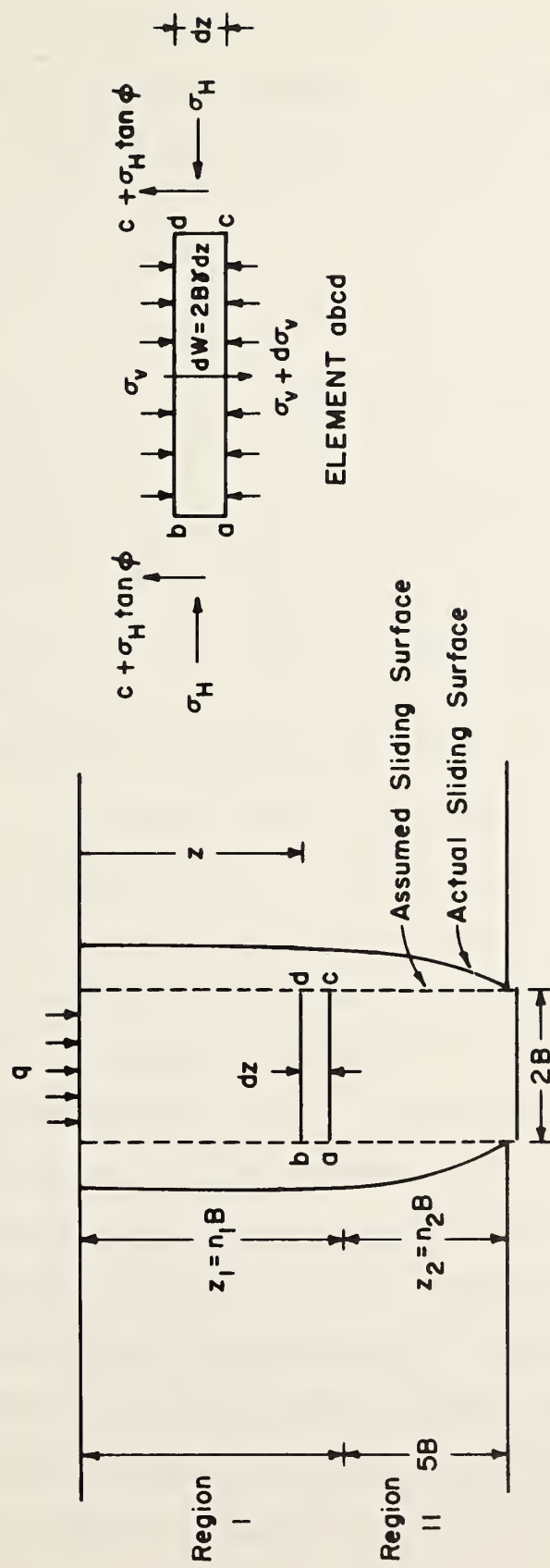
FIGURE 2.8. ARCHING ABOVE A YIELDING TRAP DOOR (AFTER TERZAGHI, 1943)

25

trap door (which Terzaghi claims is reasonable, based on his experimental work), the vertical stress σ_v acting on the trap door can be expressed approximately as:

$$\sigma_v = \frac{B\gamma}{K \tan \phi} \tag{2.2}$$

in which B = trap door half-width

γ = unit weight of soil

ϕ = friction angle of soil

The theoretical arching pressure expressed by (2.2) is not directly related to the loads acting on the tunnel supports, however. The arching of a cohesionless sand above a yielding trap door is in some respects similar to the arching of an actual soil or rock mass above a deforming tunnel support, but the two situations are not by any means precisely equivalent. For example, both the patterns and the magnitudes of the ground movements above the yielding trap door are different from the movements around the excavated tunnel. Nevertheless, from the fundamental principles in his theory and his actual observations of many (mostly timber supported) tunnels, Terzaghi was able to make an empirical extrapolation of arching theory to the practical problem of tunnel support

26

design. The basis of this extrapolation is the hypothe-
sized mechanism depicted in Figure 2.9 (Terzaghi, 1943, and
in Proctor and White, 1946). The non-rigid support condi-
tions at the sides of the tunnel are approximated by
sliding wedges that move downward and toward the excavation.
The sliding of these wedges and the deformation of the
tunnel support itself induce movements in the ground mass
that, in a manner very roughly analogous to arching above
the yielding trap door, mobilize some of its shearing
resistance. Based on this idealization and his field ob-
servations, Terzaghi found that the pressure acting on
the tunnel support could be expressed in terms of the
equivalent overburden height, H_p:

$$H_p = C(B + H_t) \tag{2.3}$$

The factor C is an empirically derived coefficient that
varies for different ground conditions and different amounts
of support deformations.

In order to use Terzaghi's empirical arching mechan-
ism for tunnels to explain the loosening phenomenon,
it must be further extrapolated to the condition of very
large support and ground movements. As the support and
the ground behind it deforms, the ground's shearing re-
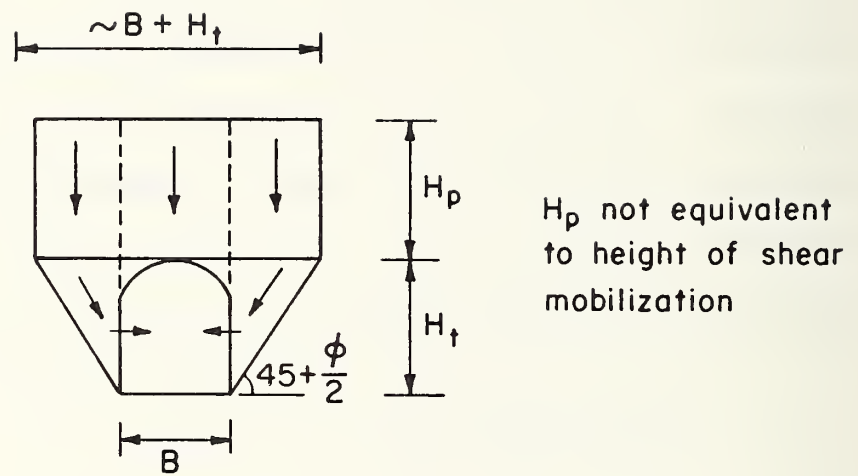sistance is mobilized and the internal cavity or support

27

FIGURE 2.9. ARCHING ABOVE A TUNNEL (AFTER TERZAGHI, 1943)

pressure needed to maintain equilibrium can be diminished -- i.e., the support load is reduced. At sufficiently large movements the maximum amount of ground resistance will be mobilized and a corresponding minimum required support pressure will be reached. This minimum support load can be thought of as corresponding to the limiting condition in which a stable "ground arch" has formed and the material beneath this arch has dropped out due to gravity forces and is now resting on the support (see Figure 2.10a). Although Terzaghi's method does not in general apply to this limiting condition, observations in actual tunnels do bear out this idealized behavior (for example, see the data from the Kielder Experimental Tunnel in Figure 2.11). Since loosening is theorized to occur only at large ground deformations (which is in a way sub-stantiated by the fact that it has never been observed at the small to moderate levels of deformation in actual tun-nels), it should be closely related to this limiting condition of gravity loading beneath a stable ground arch.

Actually, the situation depicted in Figure 2.10a is only half of the picture. For all tunnels except those at shallow depths, the stresses and displacements at points away from the tunnel are roughly symmetric about the horizontal axis. Therefore, instead of a "ground arch" forming above the tunnel as in Figure 2.10a, a symmetric
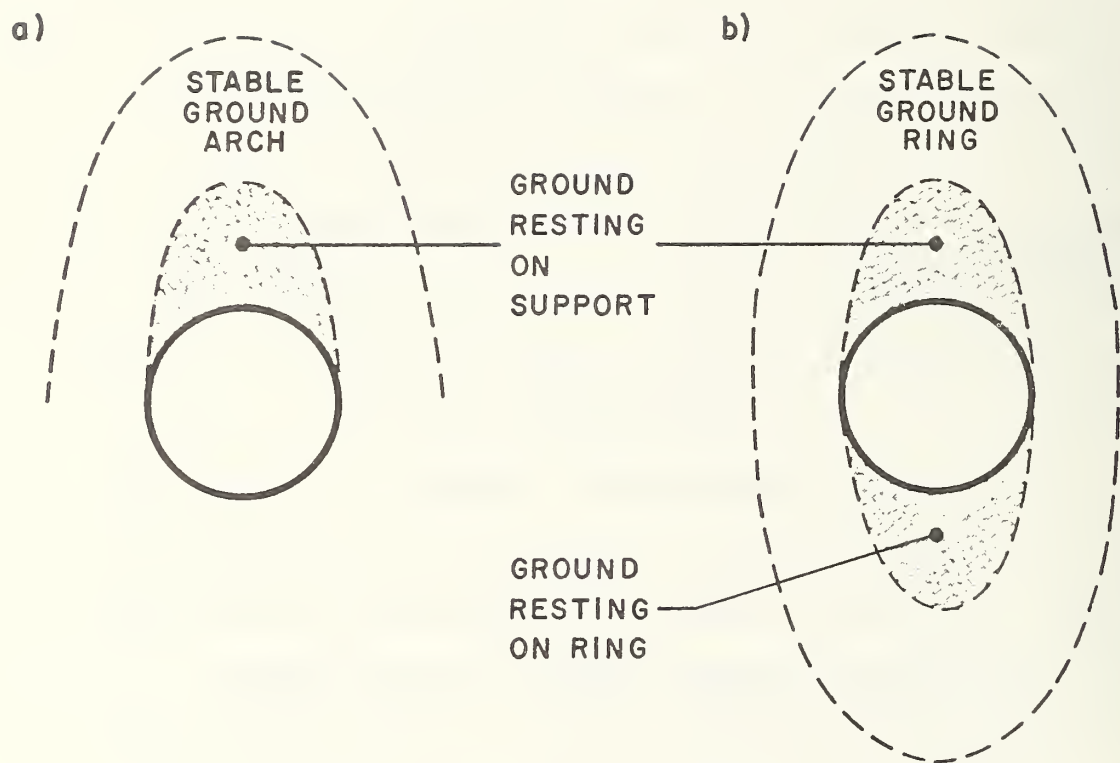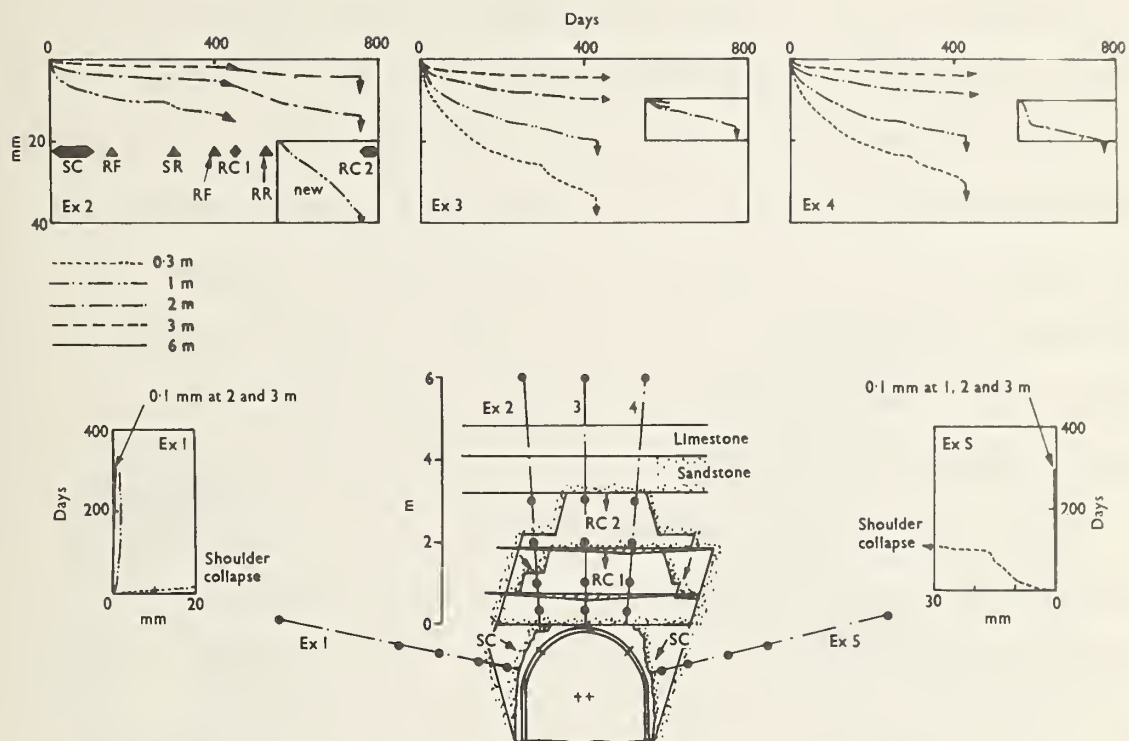
29

FIGURE 2.10.   LIMITING CASES FOR ARCHING AROUND A TUNNEL

Layout of extensometers (EX 1 to 5), their anchor positions, the shoulder collapse SC and the two roof collapses RC1 and RC2. The graphs on the top and sides show the rock displacement–time plots at each anchor position

FIGURE 2.11.   OBSERVED ROOF COLLAPSES IN THE KIELDER EXPERIMENTAL TUNNEL (FROM WARD, 1978)

"ground ring" develops and completely surrounds the tunnel as in Figure 2.10b. The tunnel support must sustain the forces in the ground within this stable ring. However, since the forces on the material within the stable ring are primarily due to gravity in this limiting case, the support must only sustain the weight of the material "resting" on the crown; the material below the invert "rests" on the ground ring. For practical purposes, then, the "arch" in Figure 2.10a is equivalent to the "ring" in Figure 2.10b.

Up to this point, the discussion of the limiting condition of a stable ground arch has not implied the existence of loosening. If anything, it has implied just the opposite -- if the arch is truly stable, the support must sustain only the weight of the material beneath the arch regardless of how much the support displacement is increased. In terms of characteristic curves, this implies that the ground curve becomes horizontal; the ground curve does not sweep upward and there is no loosening range.

However, there is reason to believe that in some cases a stable ground arch does not form for the limiting condition of large displacements. Rabcewicz (1969) has theorized that, as the ground arch forms, stress concentrations develop at the tunnel springlines until wedge-shaped "shear bodies" form and slide into the tunnel (see Figure 2.12a). These shear bodies have been observed

32

a) FORMATION OF
SHEAR BODIES

b) NEW GROUND ARCH
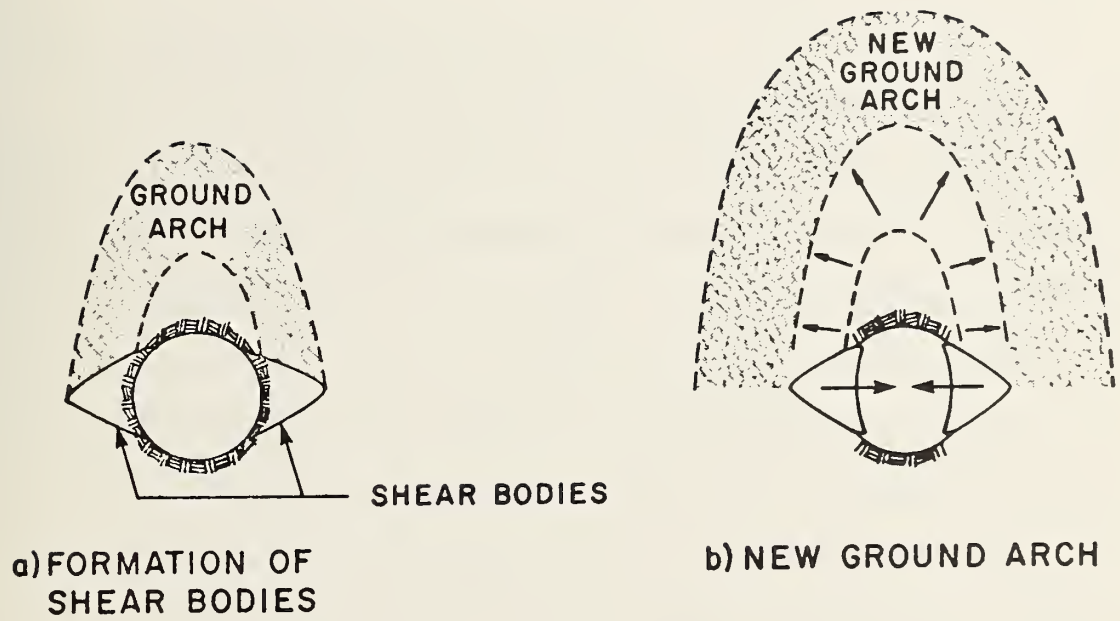
FIGURE 2.12.   FORMATION OF SHEAR BODIES AT TUNNEL SPRINGLINES

in some of the Trans-Iranian Railroad tunnels (Rabcewicz, 1962), in the Navajo Tunnel No. 3 (Sperry and Heuer, 1972) and in scale model tests (Heuer and Hendron, 1971). The effect of the movement of these shear bodies into the tunnel is that the "abutments" of the ground arch yield before the arch has fully stabilized; as these abutments yield, a new ground arch must form farther from the opening (Figure 2.12b). This new arch will be wider and higher than the original and, assuming that this new arch will fully stabilize after additional displacements, the weight of the material resting on the support will have increased -- i.e., loosening will have developed.

Of course, the potential now exists for progressive failure, especially if the ground is strain softening. New and larger shear bodies may develop as soon as the new ground arch forms, thus causing the ground arch to move out even farther. On the other hand, the applied shear stress may be lower and the ground resistance higher for the new, larger ground arch and shear bodies, and the process may stabilize. It is at this point where the theory begins to break down. There is no way to predict on the basis of these highly idealized mechanisms whether or not progressive yielding at the arch abutments will develop or, even more fundamentally, what influence this yielding will really have on the ground arch formation.

The very concept of the stable ground arch is an extension
of Terzaghi's empirical arching mechanism around tunnels
that in turn was an extrapolation of his original arching
theory and trap door experiments. To now extend this
theory another large step would at best be highly specula-
tive.

2.4.3 Conclusions About Loosening

Neither the extrapolated implications of arching
theory nor the very approximate and contradictory results
from strain softening plastic continuum theory definitively
settle the question of loosening. Although the arguments
are conceptually plausible, they contain too many unsub-
stantiated assumptions and approximations to be used to
make rational design decisions. The only reasonably con-
sistent conclusion throughout all of the arguments is
that loosening only occurs at very large deformations, much
larger than those that develop in most practical tunneling
situations, but even this conclusion cannot be verified.
Designers can find solace in the only certain fact that
is known about loosening, however: as stated by Ward
(1978) in his Rankine lecture, "The field evidence for
such [loosening] behavior has not been found ... either in
the literature or in construction projects in deep
tunnels in quite a variety of weak rocks." (pg. 161)

2.5   DEVELOPMENT OF THE FAILURE ZONE

So far, the mechanisms underlying failure in the ground mass have been discussed. What be done now is to consider the load redistribution and ground movement occurring around a tunnel in order to obtain a complete conceptual model of the development of the failure zone around tunnels.

Failure of the ground occurs when the applied shear stresses exceed the shear strength of the material. In other words, failure results when the difference between the major and minor principal stresses exceeds some maximum allowable value. In an unlined tunnel, the largest principal stress difference occurs at the tunnel wall where the radial stresses tend toward zero; therefore, failure will occur first at those locations on the wall where the tangential stresses (and thus the stress differences) in the ground are the largest. The largest tangential stresses in the ground mass occur in the central region of the face and at the tunnel walls a short distance behind the face. The shape of the failure zone around the advancing tunnel will then be similar to that shown in Figure 2.13a . Furthermore, if the lateral stress ratio K is less than 1, the tangential stresses at the tunnel springlines will be greater than those at the
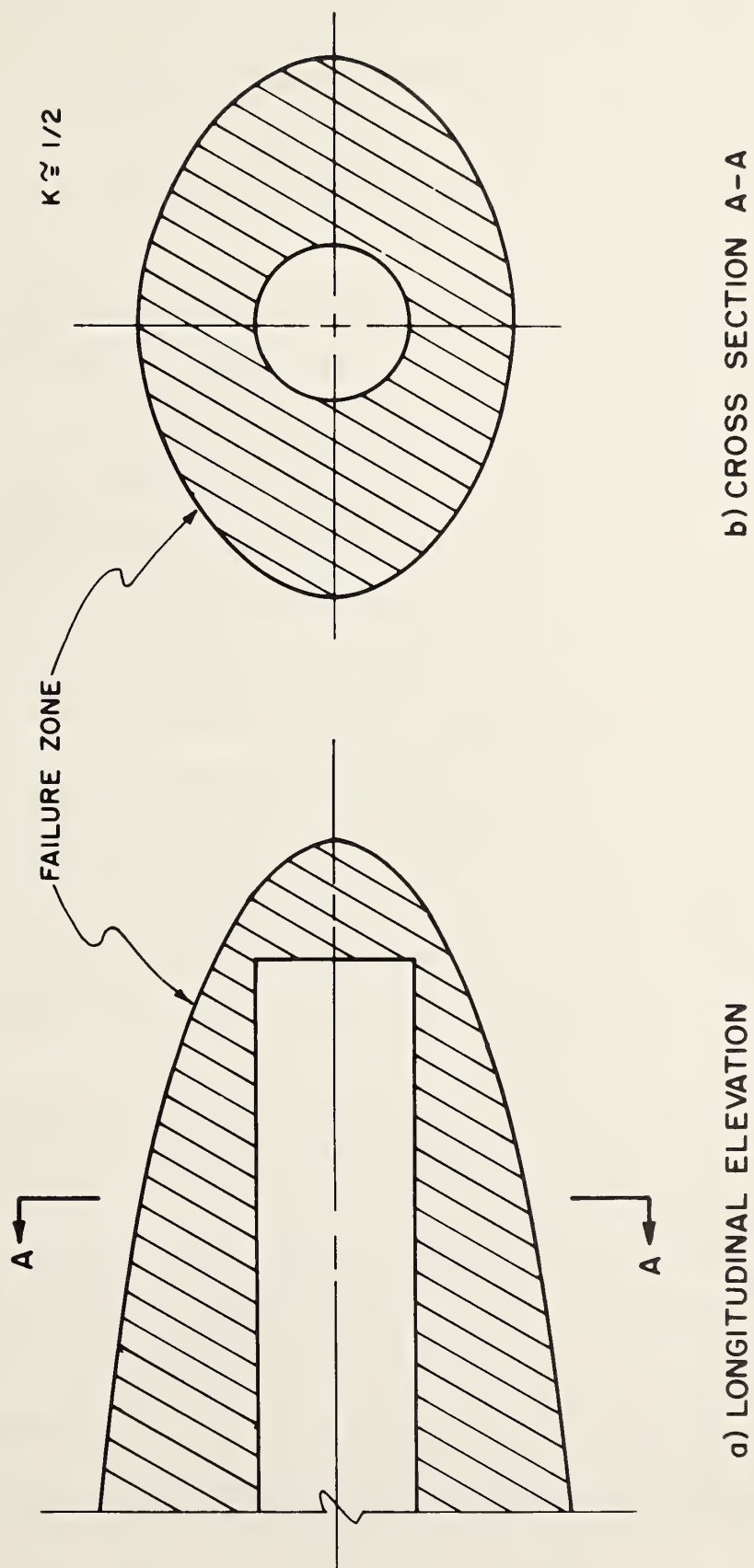
36

K ≅ 1/2

b) CROSS SECTION A-A

FAILURE ZONE

A→

A→

a) LONGITUDINAL ELEVATION

FIGURE 2.13.   EXTENT OF THE YIELDED ZONE

37

crown and invert. The ground at the springlines will
thus yield first and the failure zone will progagate
deeper into the ground mass in the horizontal than in
vertical directions, as shown in Figure 2.13b for a value
of K of approximately 1/2.

The development of the failure zone at a specific
vertical reference plane in the ground mass as the advanc-
ing tunnel approaches is illustrated in Figure 2.14. The
longitudinal profile of the failure zone as excavation
progresses is shown on the left side of the figure while
the corresponding shape of the zone at a reference plane
A-A is shown on the right. Initially (Figure 2.14a),
the tunnel is far enough away that the ground at A-A is
unaffected and still in an unyielded condition. As the
tunnel approaches to a distance of a few diameters, however,
there begins a slight axial unloading and a corresponding
radial contraction of the ground mass at A-A. These
movements are generally small and the ground will still
remain in the elastic range.

Further advance of the tunnel face causes the begin-
ning of failure in the ground mass at plane A-A (Figure
2.14b). As the face approaches, the axial unloading in-
creases at an increasing rate. The vertical loading is
still very close to its initial value of P, but the hori-
zontal stresses in the longitudinal direction have dropped
from their original values of KP to near zero. By the time
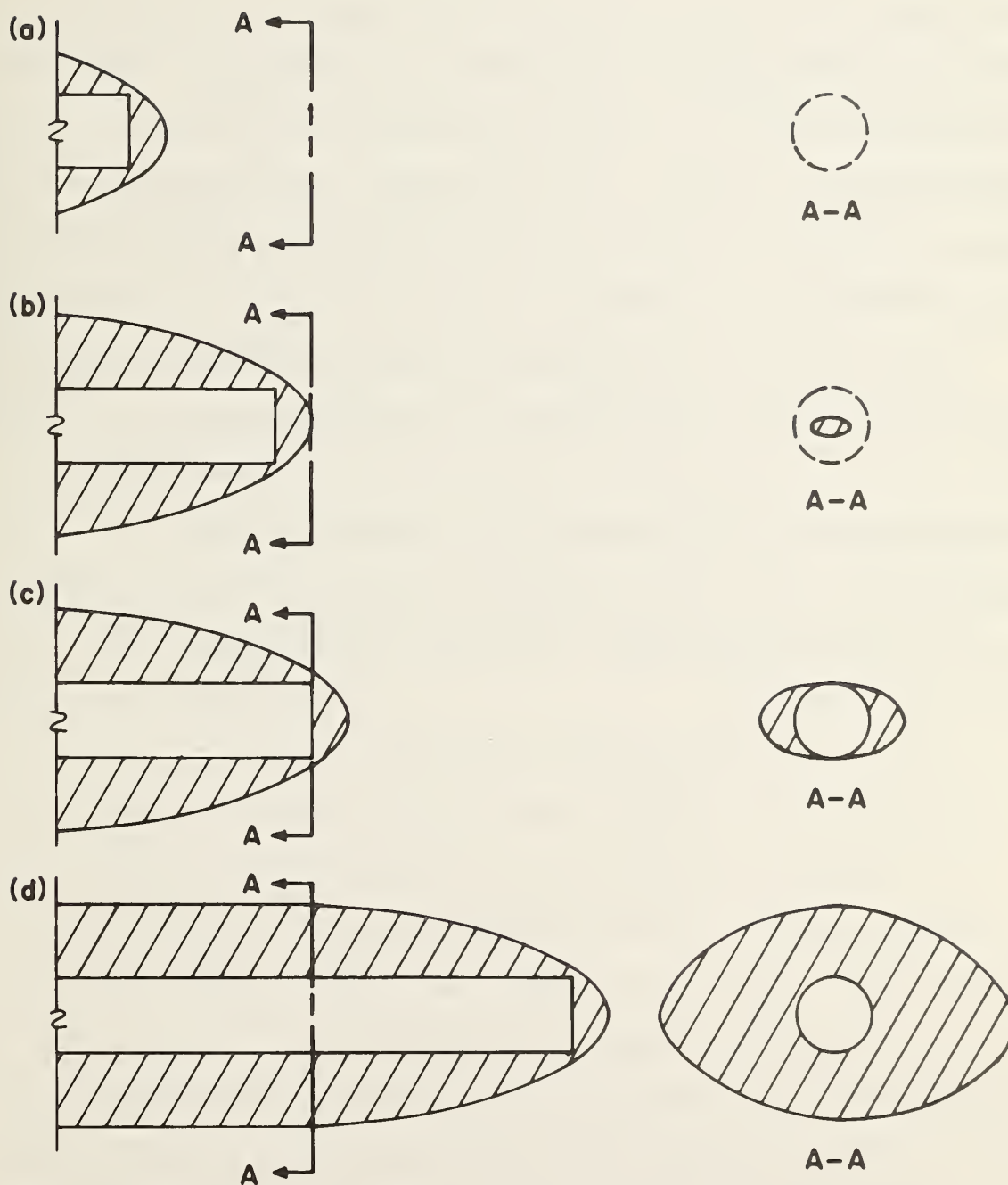
FIGURE 2.14.   DEVELOPMENT OF THE YIELDED ZONE AROUND AN
              ADVANCING TUNNEL

the face has reached the reference plane (Figure 2.14c),
the failure zone has developed its characteristic ellipti-
cal shape (for $K \cong 1/2$). The partial support provided by
the unexcavated material ahead of the face still inhibits
the full development of the failure zone, however. The
effect of this partial support decreases with further
advances of the tunnel, and the failure zone gradually
enlarges until it reaches its final extent in the plane
strain zone (Figure 2.14d).

This qualitative analysis of the development of the
yielded zone around the tunnel is substantiated by
the results of axisymmetric elasto-plastic finite element
analyses performed by Daemen and Fairhurst (1972),
Descoeudres (1974), and Ranken and Ghaboussi (1975), and
by the analyses described in Section 5 of Volume I of
this report series.

3. BEHAVIOR OF CYLINDRICAL TUNNELS IN
STRAIN-SOFTENING GROUND

This Section presents a closed-form solution for predicting displacements, strains and stresses around a circular opening in a strain softening medium. Specifically, uniform unloading in a homogeneous isotropic "linearly elastic-strain softening" infinite medium is modeled and gravity forces are neglected. Like all the solutions presented in Chapter 4 of Volume 1, the one presented herein is based on the following idealizations:

(1) plane strain

(2) free field principal stresses are equal, i.e., K=1. The tangential stress, σ_θ, and the radial stress, σ_r, are thus the major and minor principal stresses, respectively, and the problem is one-dimensional.

(3) the ground mass obeys the Tresca yield criterion

(4) ground stresses do not vary over the height of the opening. However, unlike most of the solutions presented earlier which assume elastic-perfectly plastic strength models for the ground, this assumes that the stress-strain relationship of the ground mass can be idealized as shown in Figure 3.1. If the strains resulting from unloading the ground mass are smaller than those required to mobilize the peak strength, C_p, the stress-strain relation is elastic (zone III). Once the peak strength has been reached, a further increase in strains will be accompanied by a decrease in the resistance (strain softening,
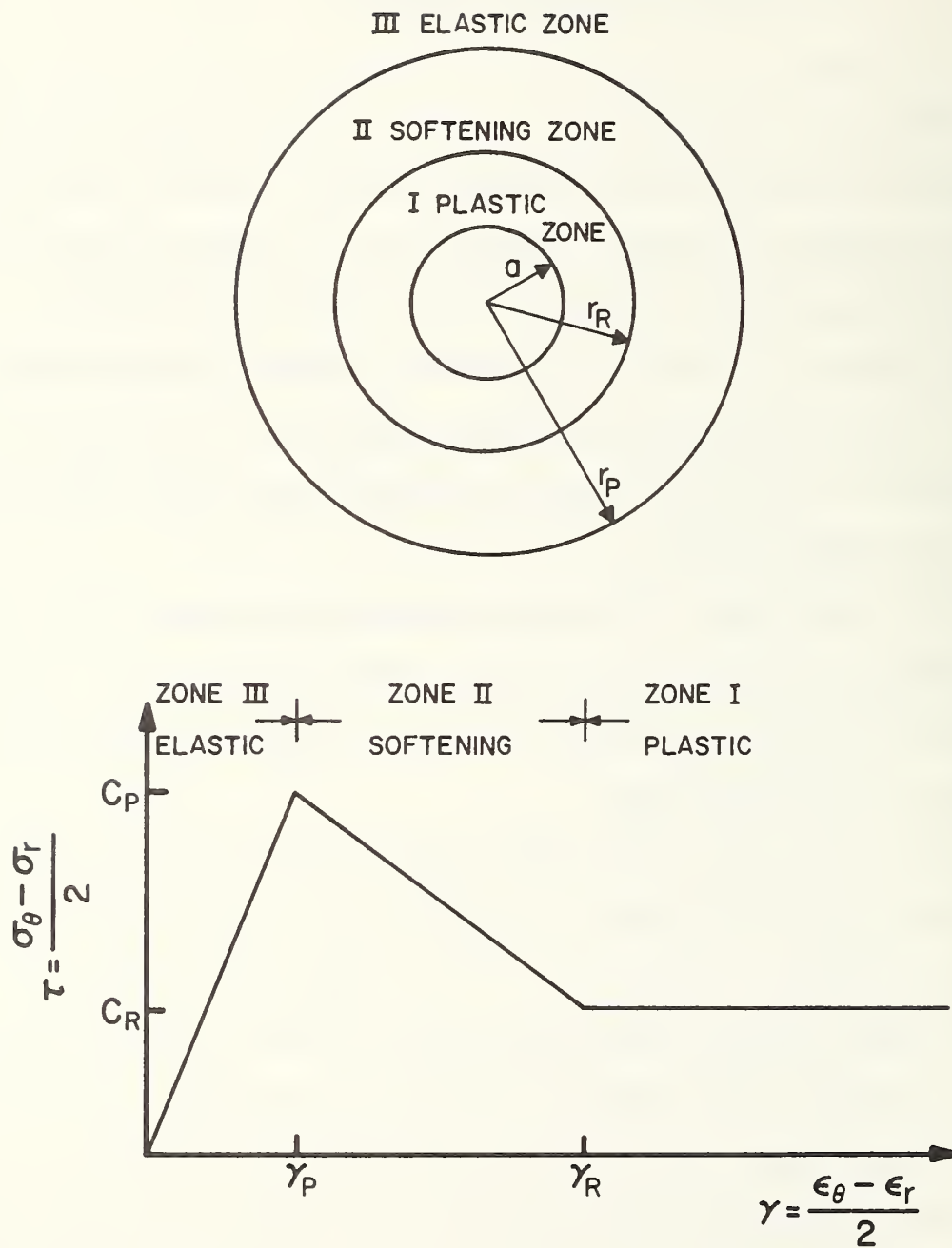
41

FIGURE 3.1   MODEL USED FOR ANALYSIS

42

zone II) until the strains are large enough to reduce the resistance to its residual value, C_R. In zone I (perfectly plastic zone), the resistance is constant, equal to C_R, and is independent of the state of strain. Choosing a cylindrical coordinate system in which r denotes the radial distance from the center of the tunnel, the material is in a plastic state within the region, $a \leq r \leq r_P$, in which a and r_P are the radii of the tunnel and the plastic zone, respectively (Figure 3.1). Furthermore, as was described above, the plastic region is divided into two zones depending on the state of strain within that zone. For $a \leq r \leq r_R$, the strains due to tunnel excavation are large enough to reduce the resistance to its residual value. For $r_R \leq r \leq r_P$, the ground is in a strain softening state. Beyond the plastic domain ($r > r_P$), the material is in an elastic state.

The stress-strain relationship governing the behavior of the ground mass can thus be expressed as follows.

a. Zone III (elastic):

$$\frac{\sigma_\theta - \sigma_r}{2} = \frac{C_P}{\gamma_P} \gamma \qquad\qquad 0 \leq \gamma \leq \gamma_P \qquad\qquad (3.1a)$$

b. Zone II (strain softening):

$$\frac{\sigma_\theta - \sigma_r}{2} = C_P - (\frac{\gamma - \gamma_P}{\gamma_R - \gamma_P})(C_P - C_R) \quad \gamma_P \leq \gamma \leq \gamma_R \qquad (3.1b)$$

c. Zone I (perfectly plastic):

$$\frac{\sigma_\theta - \sigma_r}{2} = C_R \qquad\qquad \gamma \geq \gamma_R \qquad\qquad (3.1c)$$

43

in which γ_P and γ_R are the peak and residual maximum shear strains, respectively. Furthermore, equilibrium in the aforementioned three zones requires that the stresses satisfy the relation (for axisymmetric or K=1 condition):

$$\frac{d\sigma_r}{dr} = \frac{\sigma_\theta - \sigma_r}{r} \qquad (3.2)$$

The solution is obtained by integrating Eqs. (3.2) with the constraint that σ_θ and σ_r are related through Eq. (3.1) and that the radial stresses and displacements are continuous at the boundaries between the different layers.

3.1   RELATIONS FOR THE ELASTIC ZONE

3.1.1   Stresses

In the elastic zone, the stresses are given by the familiar expressions (see Obert and Duvall,1974, for example):

$$\sigma_r = P_o - \frac{B}{r^2} \qquad (3.3a)$$

$$\sigma_\theta = P_o + \frac{B}{r^2} \qquad (3.3b)$$

in which P_o is the far-field in situ stress. The constant B is determined from the condition that at $r = r_p$ the stresses must satisfy the Tresca yield criterion, which requires that:

$$\frac{\sigma_\theta - \sigma_r}{2} = C_p \qquad (3.4)$$

44

Combining Eqs. (3.3) with (3.4), one obtains:

$$B = c_p r_p^2 \tag{3.5}$$

The stresses in the elastic zone are then given by:

$$\sigma_r = P_o - c_p \frac{r_p^2}{r^2} \tag{3.6a}$$

$$\sigma_\Theta = P_o + c_p \frac{r_p^2}{r^2} \tag{3.6b}$$

3.1.2 Displacements

The radial and tangential strains can be stated in terms of the radial displacement (positive into rock mass), u, as follows:

$$\varepsilon_r = - \frac{du}{dr} \tag{3.7a}$$

$$\varepsilon_\Theta = - \frac{u}{r} \tag{3.7b}$$

Furthermore, within this elastic zone, the stresses and strains are related by the following constitutive relations:

$$\varepsilon_r = \frac{\sigma_r}{E} - \frac{\nu}{E} (\sigma_\Theta + \sigma_z) \tag{3.8a}$$

$$\varepsilon_\Theta = \frac{\sigma_\Theta}{E} - \frac{\nu}{E} (\sigma_r + \sigma_z) \tag{3.8b}$$

in which σ_z is the stress parallel to the axis of the tunnel. For the plane strain case considered herein, this stress is given by:

$$\sigma_z = \nu (\sigma_r + \sigma_\Theta) \tag{3.9}$$

Substituting Eq. (3.9) into Eqs. (3.8), the following expressions for ε_r and ε_Θ are obtained:

$$\varepsilon_r = \frac{1+\nu}{E} [\sigma_r - \nu(\sigma_r + \sigma_\Theta)] \tag{3.10a}$$

$$\varepsilon_\Theta = \frac{1+\nu}{E} [\sigma_\Theta - \nu(\sigma_r + \sigma_\Theta)] \tag{3.10b}$$

Combining Eqs. (3.7b) and (3.10b) and noting that:

$$\frac{C_P}{\gamma_P} = 2G = \frac{E}{1+\nu} \tag{3.11}$$

in which G is the shear modulus, the radial displacement u is thus given by:

$$u = -\frac{P_o}{C_P} r \gamma_P (1-2\nu) - \gamma_P \frac{r_P^2}{r} \tag{3.12}$$

This expression for u includes the displacements due to tunnel excavation as well as the initial displacement resulting from the in situ stresses. This initial displacement, u_i, is obtained by combining Eqs. (3.7b) and (3.10b) and setting $\sigma_r = \sigma_\Theta = P_o$, i.e.,

$$u_i = -\frac{P_o}{C_P} \gamma_P r(1-2\nu) \tag{3.13}$$

Hence, the incremental radial displacement due to tunneling is obtained by subtracting u_i (Eq. 3.13) from u (Eq. 3.12), or:

$$u = -\gamma_P \frac{r_P^2}{r} \tag{3.14}$$

46

At $r = r_P$:

$$u_P = - \gamma_P \ r_P \qquad (3.15)$$

3.2 RELATIONS FOR THE YIELDED ZONE

3.2.1 Displacements

The radial displacements at the tunnel wall are due to both the inelastic strains in the plastic zone adjacent to the tunnel and the elastic strains in the ground mass outside the plastic zone. The strains in the elastic zone were derived above. The calculation of the strains in the plastic zone requires an assumption relating the plastic strains and the volume change characteristics of the material. In this solution it was assumed that upon failure the material throughout the plastic zone experiences a constant volume increase which is independent of the strains within the plastic zone. This increase in volume, ΔV, is expressed as:

$$\Delta V = \bar{\epsilon}_v V \simeq \bar{\epsilon}_v \Pi \ (r_P^2 - r^2) \qquad (3.16)$$

where $\bar{\epsilon}_v$ is an empirically determined average volumetric strain in the yielded zone (positive $\bar{\epsilon}_v$ implies volumetric compression). Hence, considerations of volume change characteristics yields:

$$\Pi (r_P^2 - r^2) = \Pi [(r_P - u_P)^2 - (r-u)^2] \ - \ \Delta V \qquad (3.17)$$

Therefore, for small displacements:

$$u \simeq \frac{r_P}{r} \ u_P + \frac{\Delta V}{2 \Pi r} \qquad (3.18)$$

and from Eqs. (3.15) and (3.16):

$$u \simeq - \gamma_P \ \frac{r_P^2}{r} + \frac{\bar{\epsilon}_v}{2r} \ (r_P^2 - r^2) \qquad (3.19)$$

47

At r=a (tunnel wall),

$$u_a = - \gamma_P \frac{r_P^2}{a} + \frac{\bar{\varepsilon}_v}{2a} (r_P^2 - a^2) \qquad (3.20)$$

Substituting Eq. (3.19) in Eqs. (3.7), the radial and tangential strains within the plastic zone are given by:

$$\varepsilon_r = - \gamma_P \frac{r_P^2}{r^2} + \frac{\bar{\varepsilon}_v}{2r^2}(r_P^2 - r^2) + \bar{\varepsilon}_v \qquad (3.21a)$$

$$\varepsilon_\theta = \gamma_P \frac{r_P^2}{r^2} - \frac{\bar{\varepsilon}_v}{2r^2} (r_P^2 - r^2) \qquad (3.21b)$$

and the maximum shear strain, $\gamma = \frac{1}{2}(\varepsilon_\theta - \varepsilon_r)$, is thus given by:

$$\gamma = \gamma_P \frac{r_P^2}{r^2} - \frac{\bar{\varepsilon}_v}{2r^2} r_P^2 \qquad (3.22)$$

It should be noted that Eqs. (3.19) and (3.22) are valid throughout zones I and II, i.e., the perfectly plastic and the strain softening zones.

3.2.2   Stresses Within the Perfectly Plastic Zone

The radial stress within the perfectly plastic zone is obtained by combining the equilibrium equation (3.2) with Eq. (3.1c) and integrating:

$$\sigma_r = 2C_R \ln r + B \qquad (3.23)$$

The constant B is determined from the condition that:

$$\sigma_r = P_i \quad \text{at} \quad r = a + u_a \qquad (3.24)$$

where P_i is the internal tunnel pressure.   Hence,

$$\sigma_r = P_i + C_R \ln \left(\frac{r}{a+u_a}\right)^2 \qquad (3.25a)$$

and from Eq. (3.1c):

$$\sigma_\theta = P_i + 2C_R + C_R \ln \left(\frac{r}{a+u_a}\right)^2 \qquad (3.25b)$$

48

3.2.3 Stresses Within the Strain Softening Zone

The radial stress within the strain softening zone is obtained by combining Eqs. (3.2), (3.1b) and (3.22) and integrating:

$$\sigma_r = 2C_P \ell n \, r - 2 \, \frac{C_P - C_R}{\gamma_R - \gamma_P} \, \gamma_P \left(\frac{\bar{\varepsilon}_v}{4\gamma_P} \, \frac{r_P^2}{r^2} - \frac{1}{2} \, \frac{r_P^2}{r^2} - \ell n \, r \right) + B \tag{3.26}$$

However, using Eq. (3.6a) and setting $r = r_P$, one obtains:

$$\sigma_r = P_o - C_P \quad \text{at} \quad r = r_P \tag{3.27}$$

This yields:

$$\sigma_r = P_o - C_P + \frac{C_P \gamma_R - C_R \gamma_P}{\gamma_R - \gamma_P} \quad \ell n \left(\frac{r}{r_P} \right)^2$$

$$+ \frac{C_P - C_R}{\gamma_R - \gamma_P} \, \gamma_P \left[\left(\frac{r_P^2}{r^2} - 1 \right) \left(1 - \frac{\bar{\varepsilon}_v}{2\gamma_P} \right) \right] \tag{3.28a}$$

and from Eq. (3.1b):

$$\sigma_\Theta = P_o + C_P + \frac{C_P \gamma_R - C_R \gamma_P}{\gamma_R - \gamma_P} \, \ell n \left(\frac{r}{r_P} \right)^2$$

$$- \frac{C_P - C_R}{\gamma_R - \gamma_P} \, \gamma_P \left[\left(\frac{r_P^2}{r^2} - 1 \right) \left(1 - \frac{\bar{\varepsilon}_v}{2\gamma_P} \right) \right] \tag{3.28b}$$

3.2.4 Radii of Zones I and II

The radius of the perfectly plastic zone, r_R, is obtained by matching the radial stresses given by Eqs. (3.25a) and (3.28a) at $r = r_R$ and combining with Eqs. (3.20) and (3.22, evaluated at $r = r_R$). This produces:

49

$$r_{R/a} = [1 - \frac{\bar{\epsilon}_v}{2} + \frac{r_R^2}{a^2}(\frac{\gamma_R}{\gamma_P - \frac{\bar{\epsilon}_v}{2}})(\frac{\bar{\epsilon}_v}{2} - \gamma_P)] \ \times$$

$$\exp[\frac{P_o - P_i - C_R + \frac{C_P\gamma_R - C_R\gamma_P}{\gamma_R - \gamma_P}\ \ell n\ (\frac{\gamma_P - \frac{\bar{\epsilon}_v}{2}}{\gamma_R}) + \frac{\bar{\epsilon}_v}{2}\frac{C_P - C_R}{\gamma_R - \gamma_P}}{2C_R}]$$

<div align="right">(3.29)</div>

The relationship between r_P and r_R is obtained from Eq. (3.22) evaluated at $r = r_R$:

$$r_P = r_R\ (\frac{\gamma_R}{\gamma_P - \frac{\bar{\epsilon}_v}{2}})^{1/2}$$

<div align="right">(3.30)</div>

3.3 SPECIAL CASES

3.3.1 Solution for a Two-Zone Material

The first step in using this solution to predict the behavior of a circular tunnel in a strain softening ground mass is to obtain the radii of the perfectly plastic zone, r_R, and the yield zone, r_P. Once these values are obtained, strains, displacements and stresses in all zones can be easily computed. However, if r_R/a from Eq. (3.29) is less than one, the perfectly plastic zone (zone I) does not develop and the behavior of the ground mass is represented by an "elastic-strain softening" stress-strain curve.

For this case, the stresses in the strain softening zone, given by Eqs. (3.28), remain the same. However, the extent of the yield zone is now obtained by equating the radial stress of the strain softening zone to the internal tunnel pressure. This yields:

$$0 = \ln\left(\frac{r_P}{a+u_a}\right)^2 - \left(\frac{r_P}{a+u_a}\right)^2 \left(\frac{C_P-C_R}{C_P\gamma_R-C_R\gamma_P}\right)\gamma_P\left(1 - \frac{\bar{\varepsilon}_v}{2\gamma_P}\right)$$

$$+ 1 - \frac{P_o-P_i}{C_P}\left(\frac{C_P-C_R}{C_P\gamma_R-C_R\gamma_P}\right)\gamma_P - \left(\frac{C_P-C_R}{C_P\gamma_R-C_R\gamma_P}\right)\frac{\bar{\varepsilon}_v}{2} \qquad (3.31)$$

This equation can be solved by trial and error to obtain the value of r_P.

3.3.2   Elastic-Perfectly Plastic Ground Mass

To extend the solution to include the elasto-plastic material, the stresses in the perfectly plastic zone, Eqs. (3.25), will be :

$$\sigma_r = P_i+C_P\ln\left(\frac{r}{a+u_a}\right)^2 \qquad (3.32a)$$

$$\sigma_\theta = P_i+2C_P+C_P\ln\left(\frac{r}{a+u_a}\right)^2 \qquad (3.32b)$$

The extent of the yield zone is found by matching Eqs. (3.6a) and (3.32a). This results in:

$$\frac{r_P}{a} = \left[1 - \gamma_P\frac{r_P^2}{a^2} + \frac{\bar{\varepsilon}_v}{2}\left(\frac{r_P^2}{a^2} - 1\right)\right]\exp[(P_o-P_i-C_P)/2C_P] \qquad (3.33)$$

3.4   RESULTS

The results of this section are presented in terms of six dimensionless parameters, defined below.

$$\frac{P_o-P_i}{C_P} \quad = \text{normalized load factor}$$

$$C_P/P_o \quad = \text{normalized peak strength}$$

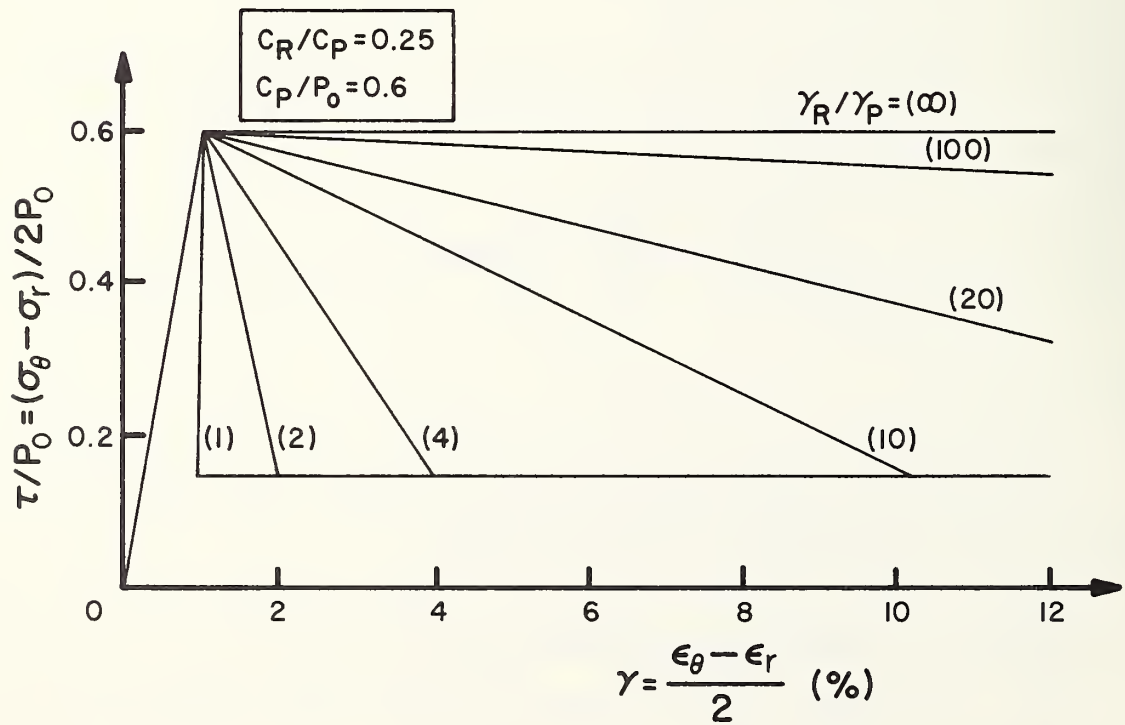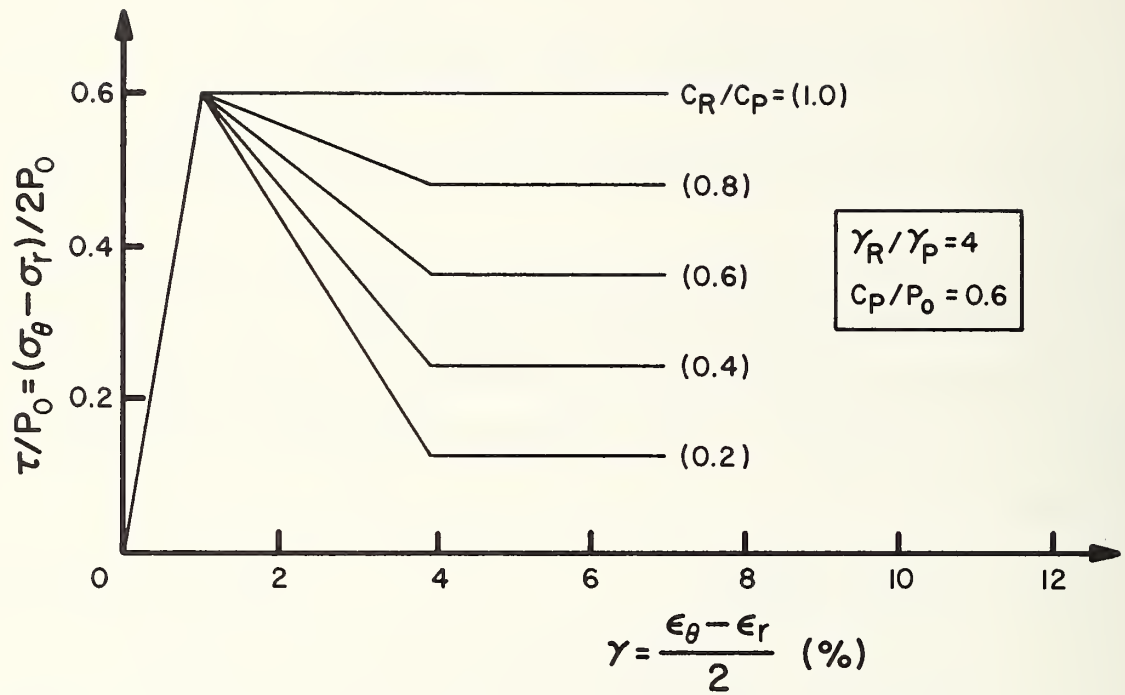$$C_R/C_P \quad = \text{strength drop ratio (see Figure 3.2)}$$

51

FIGURE 3.2   VARIATION IN STRESS–STRAIN PARAMETERS

52

γ_R/γ_P = softened strain ratio (see Fig. 3.2)

$\bar{\varepsilon}_v/\gamma_P$ = normalized volumetric strain ratio

Figures 3.3 through 3.6 give the radii of the yield zone, zone II, and the perfectly plastic zone, zone III, as a function of the normalized load factor for $\bar{\varepsilon}_v=0$ and $\gamma_P=2\%$. Figures 3.3 and 3.4 illustrate the effect of varying γ_R/γ_P on the extent of the yield zone for a fixed value of C_R/C_P (=0.5). In Figures 3.5 and 3.6, the ratio γ_R/γ_P is fixed at 2 and the influence of varying the strength drop ratio on the yield zone size is portrayed. The results in these figures show that:

1. The size of the yield zone decreases as the value of γ_R/γ_P increases (Figures 3.3 and 3.4). For a given load factor of, say, 5, the value of r_p/a in Figure 3.3 decreases from 6.15 to 4.45 as γ_R/γ_P increases from 1 (vertical drop) to ∞ (elastic-perfectly plastic ground mass). It should be emphasized that the solution presented herein was developed based on satisfying the equilibrium equation (Eq. 3.2) in the deformed geometry. Hence, the maximum displacement of the tunnel wall is equal to the radius of the tunnel, i.e., hole closure ($u_a/a=1$), thus setting an upper limit on the size of the yield zone. For the situation depicted in Figs. 3.3 through 3.6 ($\gamma_P=0.02$ and $\bar{\varepsilon}_v=0$), Eq. (3.20) gives this upper limit to be equal to 7.07 times the tunnel radius. Further discussions on this point will be made later.

2. Figures 3.5 and 3.6 show that the absolute magnitude of strength drop, C_R/C_P, has a significant effect on the size of the
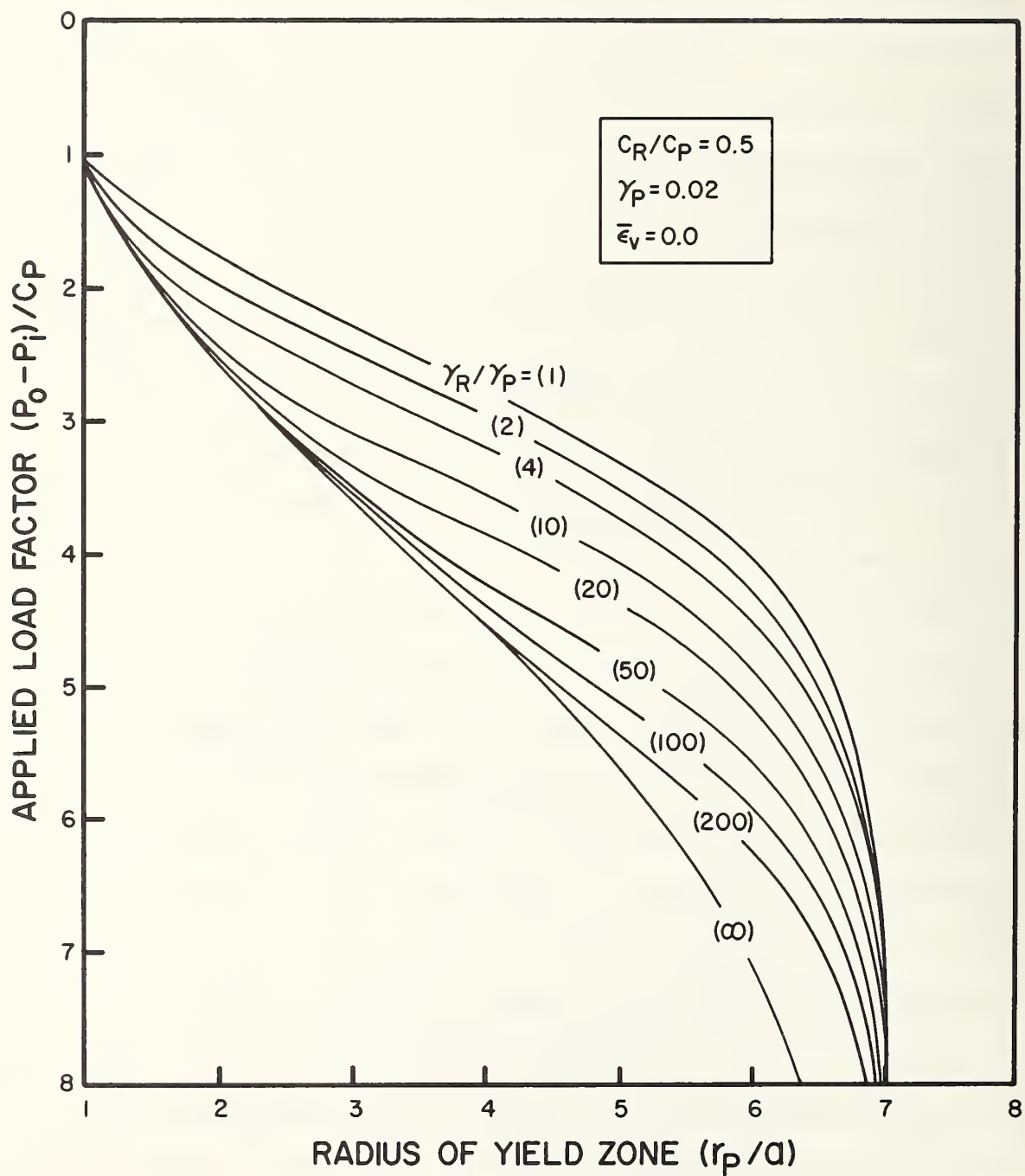
53

FIGURE 3.3   EFFECT OF STRENGTH DECAY RATE ON RADIUS OF YIELD ZONE
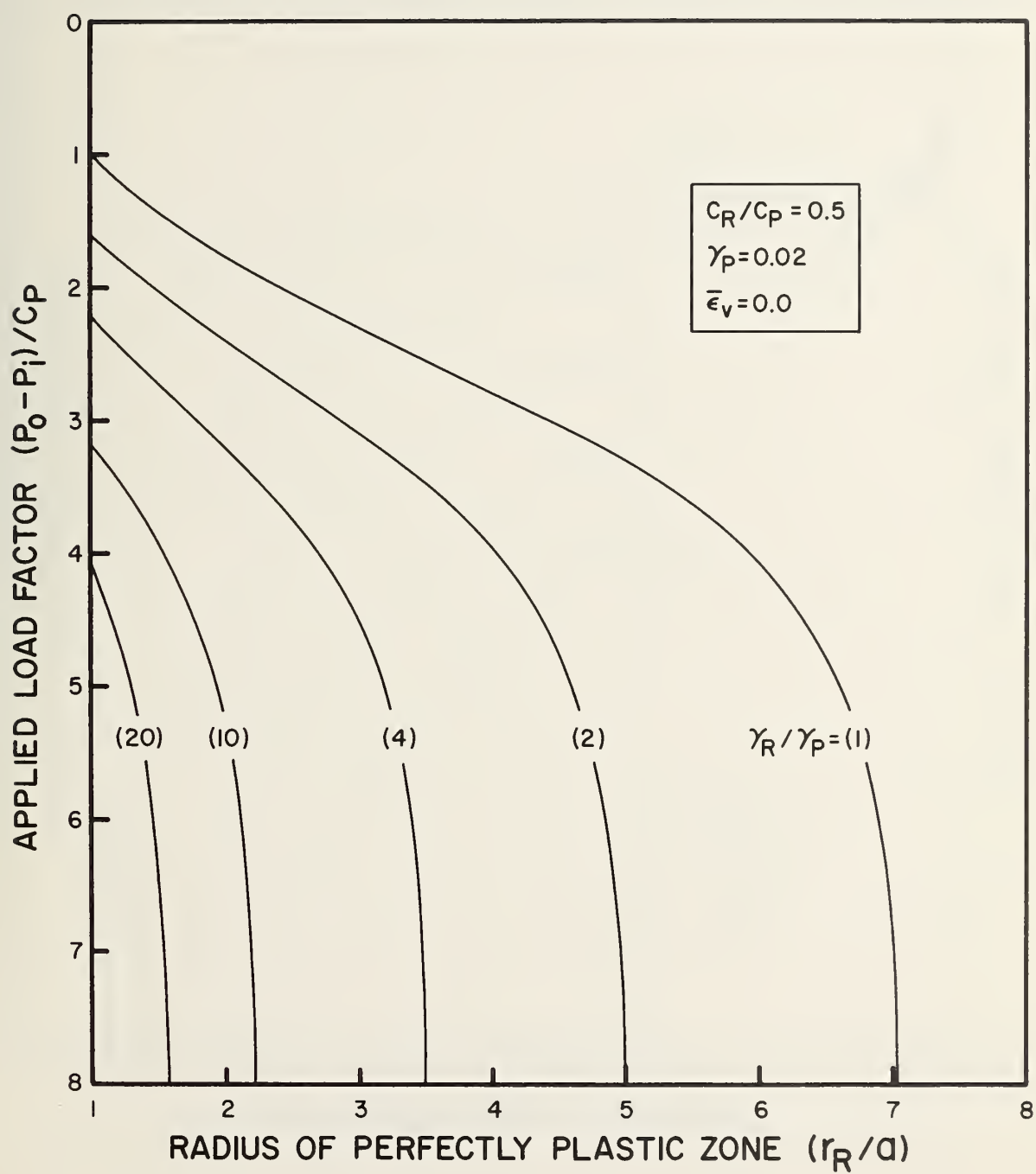
54

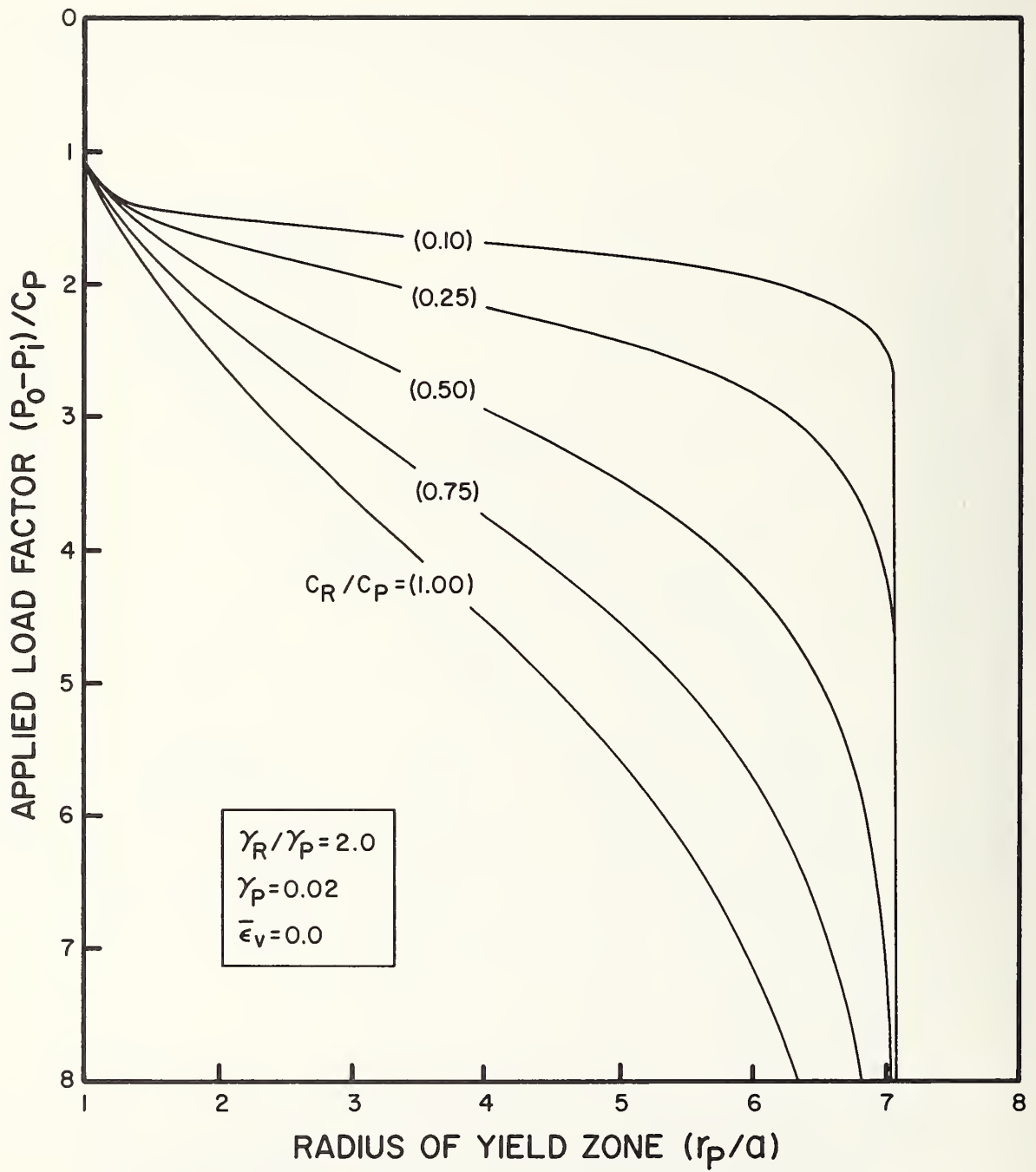FIGURE 3.4   EFFECT OF STRENGTH DECAY RATE ON RADIUS OF PERFECTLY
            PLASTIC ZONE

55

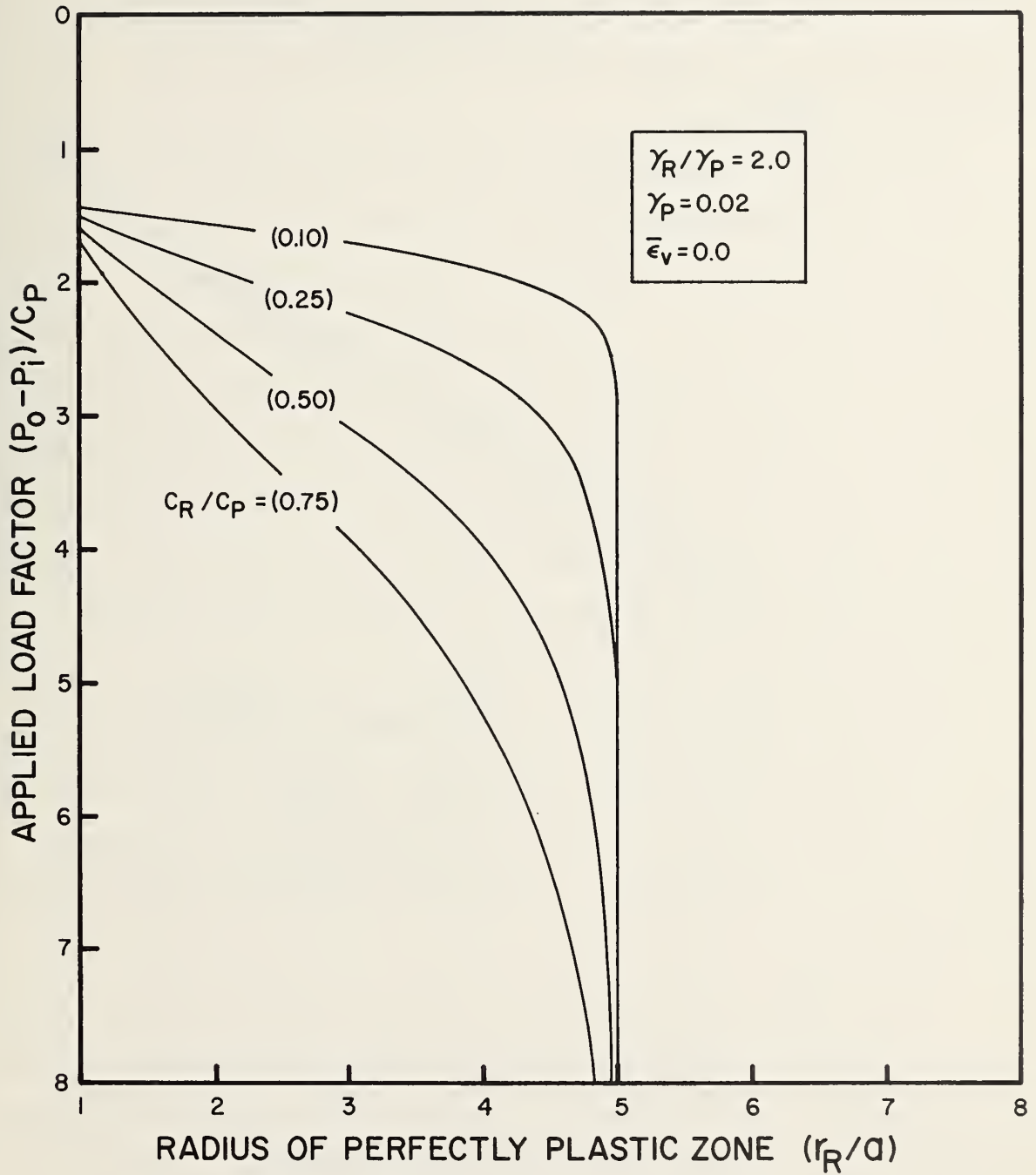FIGURE 3.5 EFFECT OF STRENGTH DROP ON RADIUS OF YIELD ZONE

56

FIGURE 3.6   EFFECT OF STRENGTH DROP ON RADIUS OF PERFECTLY
PLASTIC ZONE

57

yield zone. As the peak strength decreases in value, the amount of unloading required to close the opening becomes smaller, and in all cases yielding stops once the hole completely closes.

The effect of allowing the yield zone to change in volume (dilate) upon yielding is shown in Figure 3.7, where $(P_O-P_i)/C_P$ is plotted vs. r_p/a for $C_R/C_P=0.5$, $\gamma_R/\gamma_P=2$, $\gamma_P=2\%$ and different values of $\bar{\epsilon}_v$. It can be seen from this figure that for large amounts of unloadings (higher values of $(P_O-P_i)/C_P$), increasing the average volumetric strain, $\bar{\epsilon}_v$, reduces the size of the yield zone. This seems reasonable as the dilatent material would fill the hole sooner thus causing less yielding. However, at smaller degrees of unloading, introducing volume change increases the size of the yield zone.

Once the radius of the yielded zone is obtained, all the field variables can be easily computed. Figure 3.8 shows ground reaction curves (P_i/P_O vs. u_a/a) for materials with different stress-strain relationships. Based on this figure, the following can be concluded:

1. For the case of strain softening ground mass, curves 3 and 4, ground loosening (increase in equivalent support pressure with increasing displacements) does not occur despite the strain softening characteristics of the ground. However, this does not eliminate the possibility of loosening taking place in actual situations, since this solution is valid only under highly idealized conditions (K=1, no gravity and Tresca yield criterion).
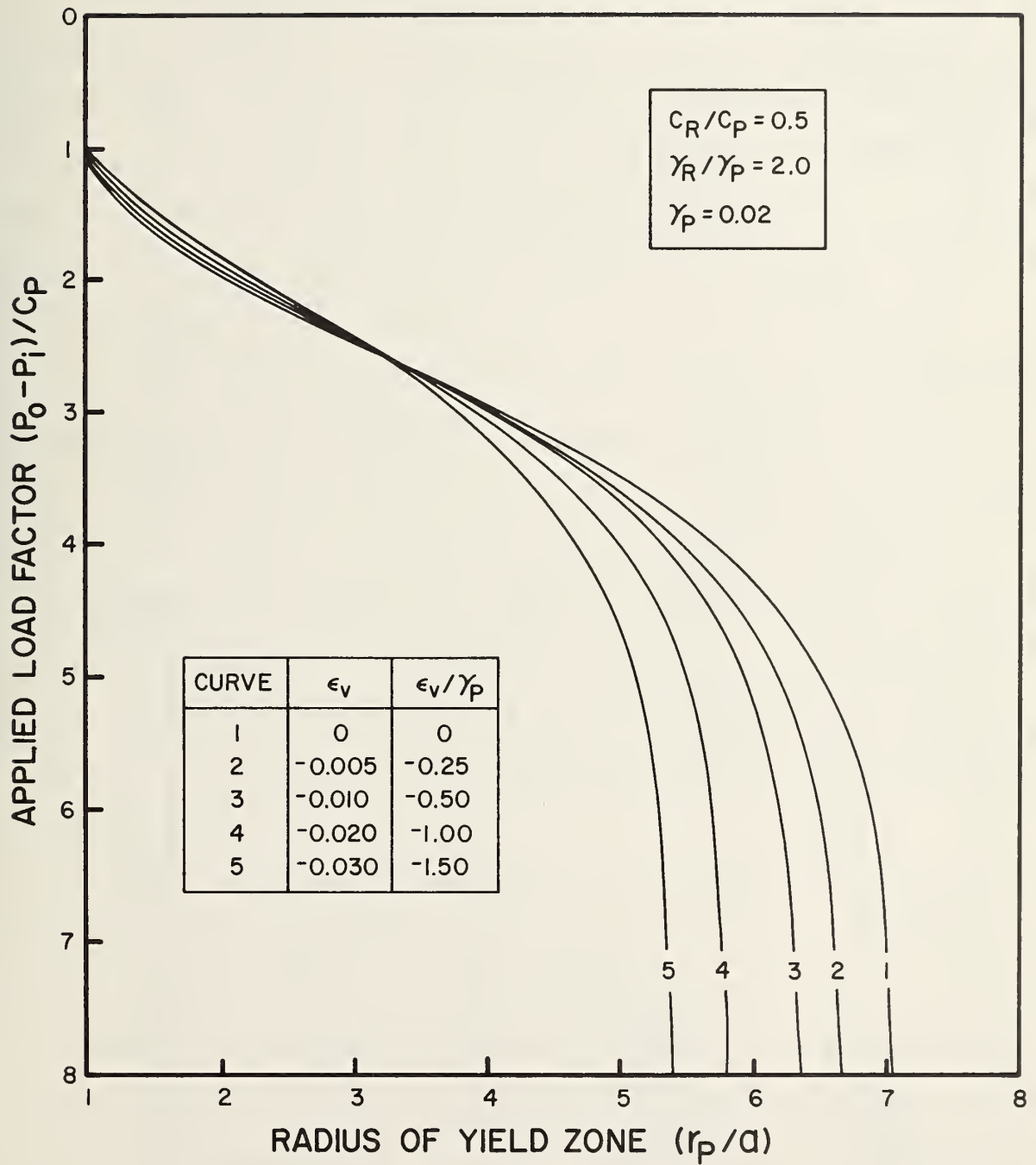
2. The dotted curves shown in this figure are based on

FIGURE 3.7   EFFECT OF STRENGTH DROP ON RADIUS OF
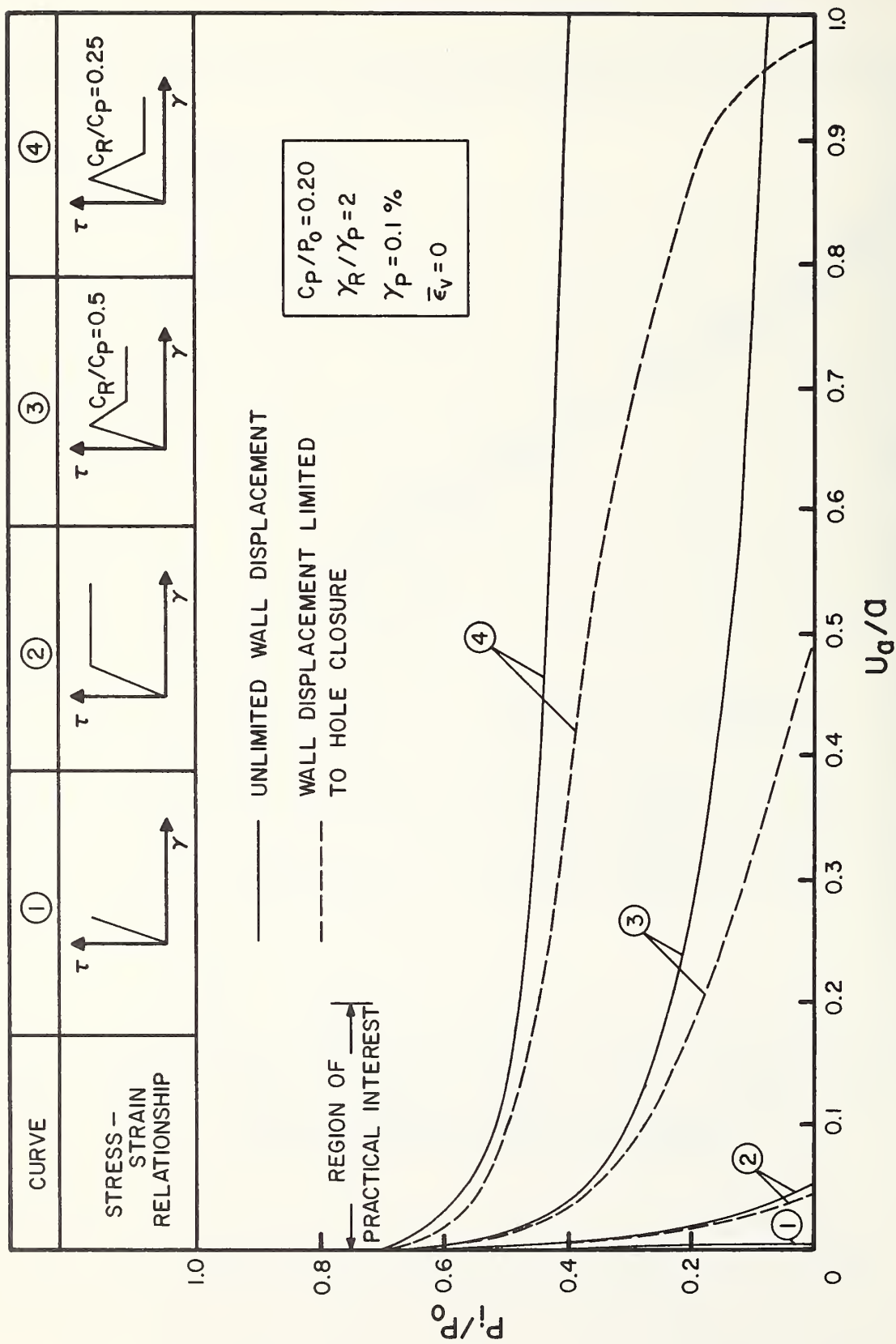PERFECTLY PLASTIC ZONE

59

FIGURE 3.8 GROUND REACTION CURVES FOR MATERIALS WITH DIFFERENT STRESS-STRAIN RELATIONSHIPS

the solution limiting wall displacements to hole closure

(i.e., satisfying equilibrium equation for the deformed

geometry). For comparison, the curves corresponding to the

solution where the equilibrium equation is satisfied for the

initial geometry (solid curves) are also shown. The comparison

shows that the two solutions deviate considerably as P_i/P_o de-

creases. However, in the region of practical interest

(u_a/a up to 20%), the solutions are close to each other.

     3.   The effect of the stress-strain relationship on the

wall displacements can be seen by comparing the four curves

shown in this figure. As the stress-strain behavior is changed

from elastic (curve 1) to elastic-perfectly plastic (curve 2)

to elastic-strain softening-perfectly plastic (curves 3 and 4),

the wall displacement significantly increases. Similarly,

decreasing the magnitude of the residual strength, C_R, relative

to the peak strength, C_p (i.e., decreasing C_R/C_p) increases the

wall displacements.

     Finally, Figures 3.9 through 3.11 give the distribution

of the principal stresses around the tunnel opening. In Figure 3.9

the distributions are given for different values of the internal

wall pressure. Three distinct zones in the σ_Θ distribution can

be easily identified. In zones I and II, perfectly plastic and

strain softening zones, σ_Θ increases with increasing the distance

from the tunnel's centerline. Once the elastic zone is reached,

σ_Θ decreases approaching the far-field in situ stress. Similar,

though less identifiable, regions also exist in the σ_r distribution.
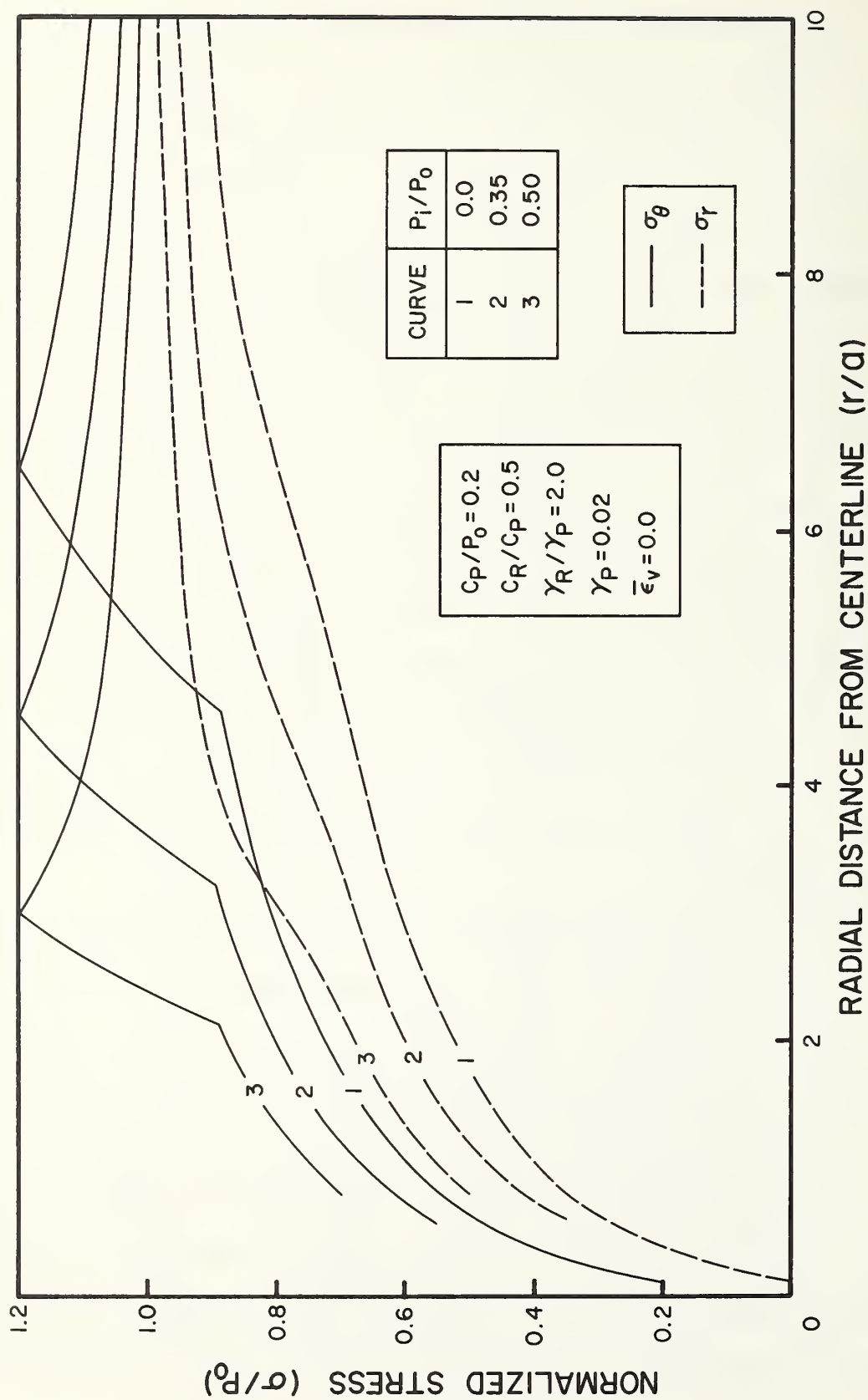
FIGURE 3.9 EFFECT OF INTERNAL WALL PRESSURE ON STRESS DISTRIBUTIONS

Chart details:

Y-axis: NORMALIZED STRESS (σ/P_0)

X-axis: RADIAL DISTANCE FROM CENTERLINE (r/a)

CURVE	P_i/P_0
1	0.0
2	0.35
3	0.50

σ_θ —— (solid)
σ_r ---- (dashed)

$C_P/P_0 = 0.2$
$C_R/C_P = 0.5$
$\gamma_R/\gamma_P = 2.0$
$\gamma_P = 0.02$
$\bar{\epsilon}_v = 0.0$
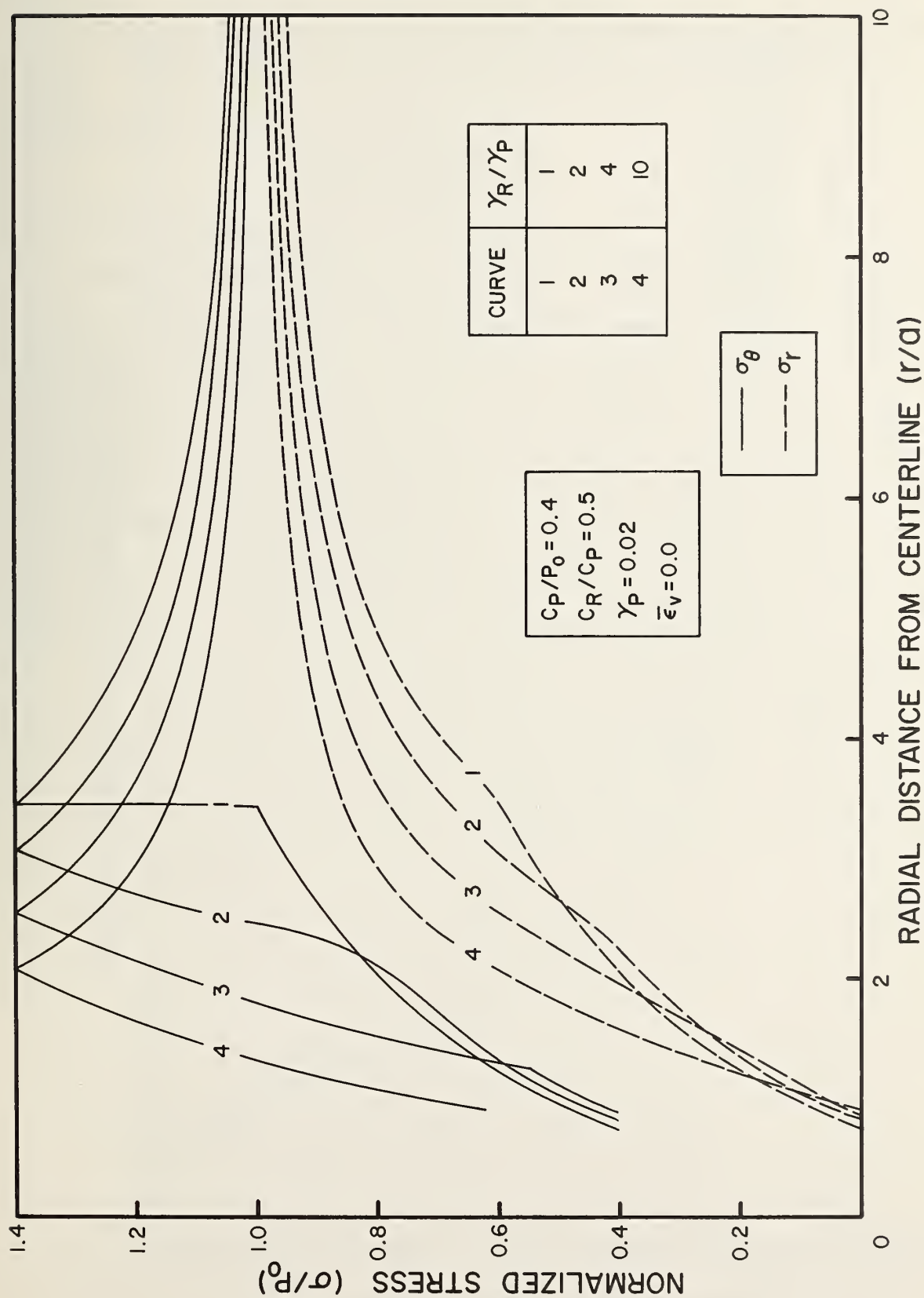
FIGURE 3.10 EFFECT OF STRENGTH DECAY RATE ON STRESS DISTRIBUTIONS
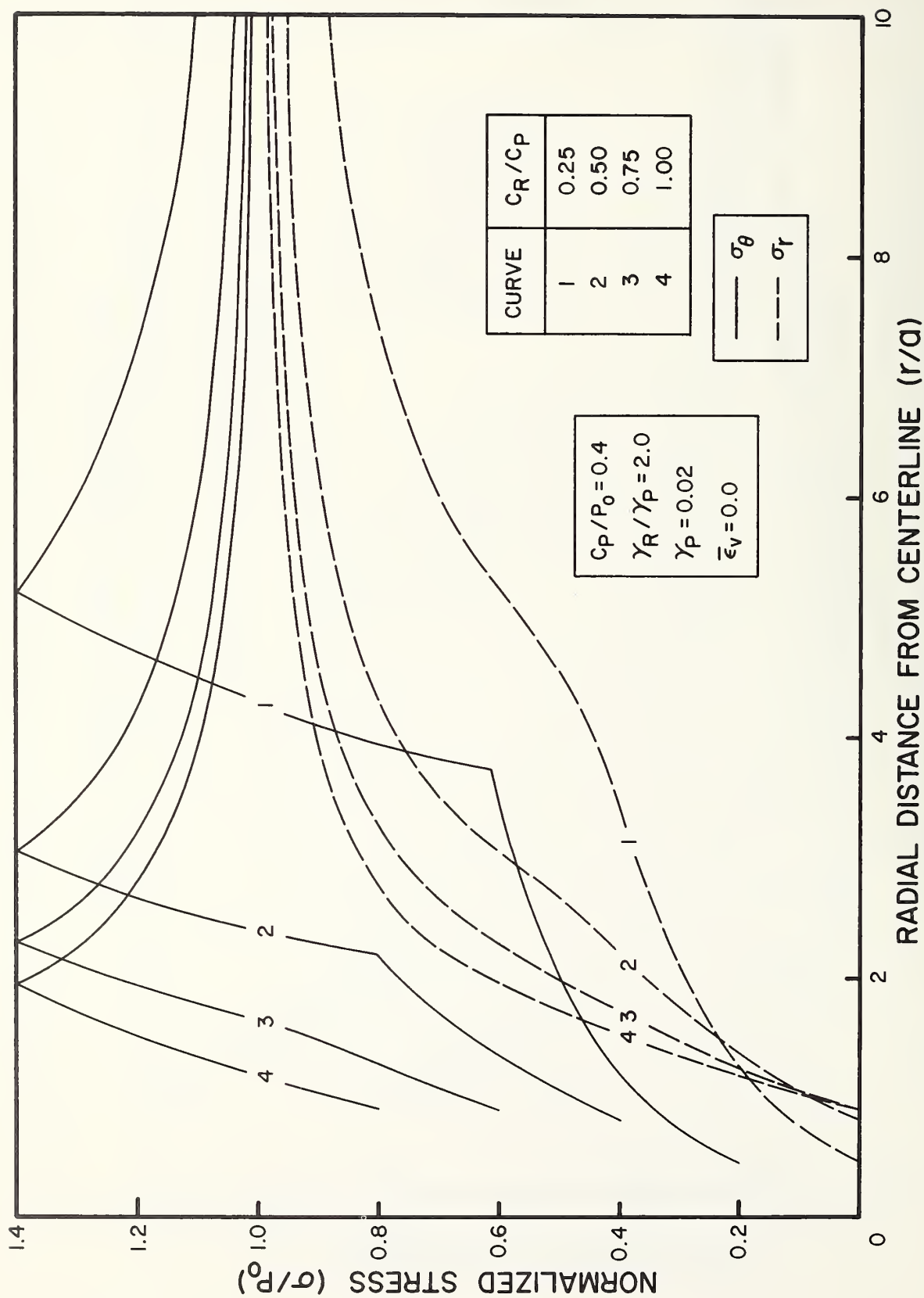
FIGURE 3.11 EFFECT OF STRENGTH DROP ON STRESS DISTRIBUTIONS

64

Figures 3.10 and 3.11 show the effect of varying γ_R/γ_P and c_R/c_P, respectively, on the stress distributions around an unsupported tunnel.

3.5 CONCLUSIONS

The analytical method described in this section provides the tunnel designer with a simple tool for analyzing strain softening behavior of the ground. Within the constraints of the simplifying assumptions, plane strain, K=1, Tresca yield criterion, the ground characteristics curves can be constructed and be used together with support reaction curves to obtain an approximate idea of ground-structure interaction in a strain softening ground. The normalized plots given in this section facilitate such studies.

In addition to providing users with an appropriate analytical method, this section also contributes to the preceding discussion on ground loosening. As was shown, strain softening behavior under the assumptions of the analysis does not cause loosening ground behavior.

4. CONCLUSIONS

The understanding of ground-structure interaction is address-
ed and improved throughout this series of reports on improved
design of tunnel supports. This particular volume has been de-
voted to a complex and ill understood aspect of ground-structure
interaction, that of ground yielding.

A conceptual review provided the reader with background on
the underlying mechanisms and the consequences of yielding ground
behavior. The often mentioned but poorly understood phenomenon
of ground loosening was subject to special consideration.
Loosening, the increase of equivalent support pressure with in-
creasing displacements (in contrast to 'normal' yielding, where the pressure
decreases with increasing displacements), can be visualized as
being caused either by strain softening ground behavior or by the
creation and displacement of a stable ground arch. Neither
mechanism is fully convincing, especially strain softening
behavior, which does not necessarily lead to ground loosening.
To further investigate this point and to provide designers with
a simple analytical tool to treat strain softening ground, a closed-
form solution was developed. The method is quite valuable,
even with the simplifying assumptions of a initially uniform
(plane strain) stress field and isotropic material properties,
which make it possible to examine in detail the effects of the
stress-strain behavior of the ground. For instance, the relative

magnitude of elastic and plastic strains, the magnitude and rate of the stress drop, and the relative magnitude of the residual resistance have significant effects on the extent of the plastic zone and on the displacements. Parametric studies and resulting graphs give the designer a firmer idea of the effects of these factors that characterize strain softening behavior. In addition, they emphasize the previously made observation, in that no loosening occurred in any of the applications of the analysis.

Although one cannot rule out loosening, the discussion in this volume has shown that it may not be as prevailing as often assumed.

We hope that with this volume, ground yielding and, as a consequence, ground-structure interaction can be better understood and analytically treated, even if some aspects remain somewhat problematic.

5. REFERENCES

Daemen, J.J.K. (1975), "Tunnel Support Loading Caused by Rock
     Failure," Technical Report No. MRD-3-75, Omaha District, U.S.
     Army Corps of Engineers, May (NTIS AD A013405).

Daemen, J.J.K. and C. Fairhurst (1972), "Rock Failure and Tunnel
     Support Loading," Proceedings, International Symposium on
     Underground Openings, Lucerne, pp. 356-369.

Descoeudres, F. (1974), "Three-Dimensional Analysis of Tunnel Stability
     Near the Face in an Elasto-Plastic Rock," Advances in Rock
     Mechanics, Proceedings, Third Congress, International Society
     for Rock Mechanics, Denver, Vol. 2, Part B, pp. 1130-
     1135 (in French).

Fenner, R. (1938), "Untersuchungen Zur Erkenntnis Des Gebirgsdruckes,"
     Glückauf, Technical Translation Report R 700159, pp. 681-695
     and 701-715.

Heuer, R.E. and A.J. Hendron, Jr. (1971), Geomechanical Model Study
     of the Behavior of Underground Openings in Rock Subjected to
     Static Loads - Report 2, Tests on Unlined Openings in Intact
     Rock, Contract Report N-69-1, U.S. Army Engineer Waterways
     Experiment Station, Vicksburg, Mississippi, February.

Obert, L. and W.J. Duvall (1967), Rock Mechanics and the Design of
     Structures in Rock, John Wiley and Sons, New York, 650 pp.

Pacher, F. (1963), "Deformationsmessungen im Versuchsstollen als
     Mittel zur Erforschung des Gebirgsuerhaltens und zur
     Bemessung des Ausbaus," Felsmechanik and Ingenieurgeologie,
     Supplementum 1, pp. 149-161.

Proctor, R.V. and T.L. White (1946), Rock Tunneling with Steel
     Supports, The Commercial Shearing and Stamping Co.,
     Youngstown, Ohio.

Rabcewicz, L.v. (1962), "Aus Der Praxis Des Tunnelbaues - Einige
     Erfahrungen Über Echten Gebirgsdruck (From the Practice of
     Tunneling - Some Experiences of True Rock Pressure),
     Geologie Und Bauwesen, Vol. 27, No. 3-4 pp. 153-167.

Rabcewicz, L.v. (1969), "The Stability of Tunnels Under Rock Load,"
     Water Power, Part 1, June, pp. 225-229; Part 2, July, pp.
     266-273; Part 3, August, pp. 297-302.

Ranken, R.E. and J. Ghaboussi (1975), Tunnel Design Considerations:
     Analysis of Stresses and Displacements Around Advancing Tun-
     nels, Report No. FRA-ORDD 75-84, Federal Railroad Administra-
     tion, U.S. Department of Transportation, August.

Sperry, P.E. and R.E. Heuer, (1972), "Excavation and Support of
    Navajo Tunnel No. 3," Proceedings of North American Rapid
    Excavation and Tunneling Conference, No. 1, Chapter 29, AIME,
    pp. 539-571.

Terzaghi, K., (1943), Theoretical Soil Mechanics, John Wiley and
    Sons, Inc., New York.

Ward, W.H., (1978), "Ground Supports for Tunnels in Weak Rocks,"
    Geotechnique, Vol. 28, No. 2, pp. 133-171.

APPENDIX

REPORT OF NEW TECHNOLOGY

The work performed under this contract has led to the development of improved practical design tools to provide more accurate representations of the ground-structure interaction in tunneling. In Section 1 of this volume, analytical treatments of ground yielding behavior are evaluated with emphasis on the problematic phenomenon of loosening. The end result of this extensive review is the development of a method for analyzing strain softening ground behavior.

71

HE 18.5 · A₃
UMTA-
Schwartz, C
Improved de
supports :

Form DOT F 1720.2
FORMERLY FORM DOT F

U.S. DEPARTMENT OF TRANSPORTATION
RESEARCH AND SPECIAL PROGRAMS ADMINISTRATION
TRANSPORTATION SYSTEMS CENTER
KENDALL SQUARE, CAMBRIDGE, MA. 02142

OFFICIAL BUSINESS
PENALTY FOR PRIVATE USE, $300

POSTAGE AND FEES PAID
U.S. DEPARTMENT OF TRANSPORTATION
613

U.S. MAIL